

École Doctorale des Sciences de l'Environnement d'Île-de-France

Année Universitaire 2014-2015

Modélisation Numérique
de l'Écoulement Atmosphérique
et Assimilation de Données

Olivier Talagrand

Cours 8

7 Mai 2015

Exact bayesian estimation ?

Particle filters

Predicted ensemble at time t : $\{x_n^b, n = 1, \dots, N\}$, each element with its own weight

(probability) $P(x_n^b)$

Observation vector at same time : $y = Hx + \varepsilon$

Bayes' formula

$$P(x_n^b|y) \sim P(y|x_n^b) P(x_n^b)$$

Defines updating of weights

Bayes' formula

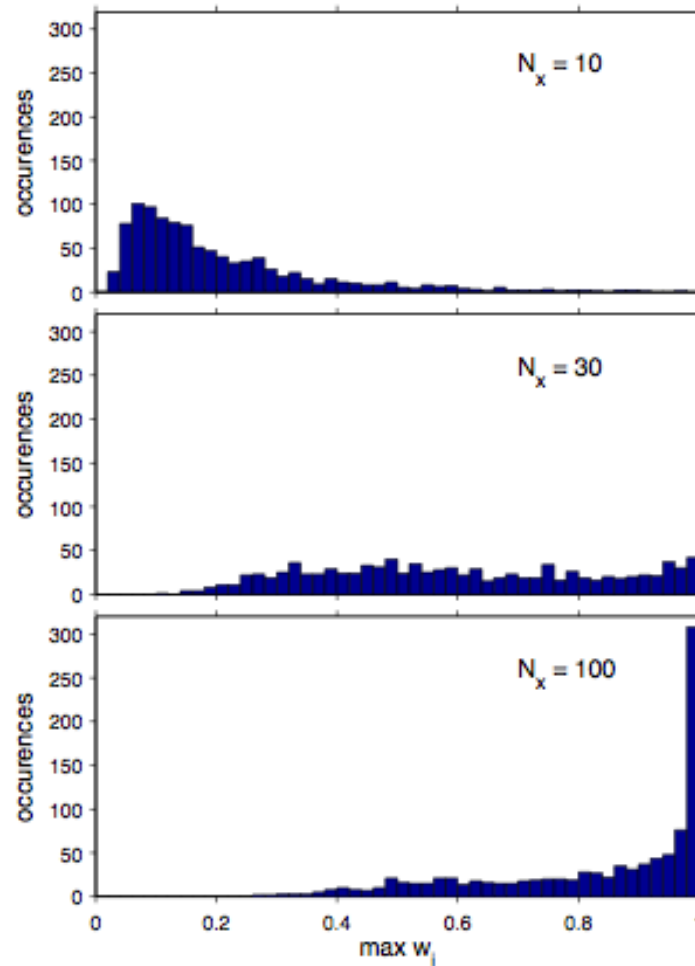
$$P(x_n^b|y) \sim P(y|x_n^b) P(x_n^b)$$

Defines updating of weights; particles are not modified. Asymptotically converges to bayesian pdf. Very easy to implement.

Observed fact. For large state dimension, ensemble tends to collapse.

Behavior of $\max w^i$

▷ $N_e = 10^3$; $N_x = 10, 30, 100$; 10^3 realizations



average squared error of
posterior mean = 5.5

... = 25

... = 127

Problem originates in the ‘curse of dimensionality’. Large dimension pdf’s are very diffuse, so that very few particles (if any) are present in areas where conditional probability (‘*likelihood*’) $P(y|x)$ is large.

Bengtsson *et al.* (2008) and Snyder *et al.* (2008) evaluate that stability of filter requires the size of ensembles to increase exponentially with space dimension.

Alternative possibilities (review in van Leeuwen, 2009, *Mon. Wea. Rev.*, 4089-4114)

Resampling. Define new ensemble.

Simplest way. Draw new ensemble according to probability distribution defined by the updated weights. Give same weight to all particles. Particles are not modified, but particles with low weights are likely to be eliminated, while particles with large weights are likely to be drawn repeatedly. For multiple particles, add noise, either from the start, or in the form of ‘model noise’ in ensuing temporal integration.

Random character of the sampling introduces noise. Alternatives exist, such as *residual sampling* (Lui and Chen, 1998, van Leeuwen, 2003). Updated weights w_n are multiplied by ensemble dimension N . Then p copies of each particle n are taken, where p is the integer part of Nw_n . Remaining particles, if needed, are taken randomly from the resulting distribution.

Importance Sampling.

Use a *proposal density* that is closer to the new observations than the density defined by the predicted particles (for instance the density defined by EnKF, after the latter has used the new observations). Independence between observations is then lost in the computation of likelihood $P(y|x)$ (or is it not ?)

In particular, *Guided Sequential Importance Sampling* (van Leeuwen, 2002).
Idea : use observations performed at time k to resample ensemble at some timestep anterior to k , or ‘nudge’ integration between times $k-1$ and k towards observation at time k .

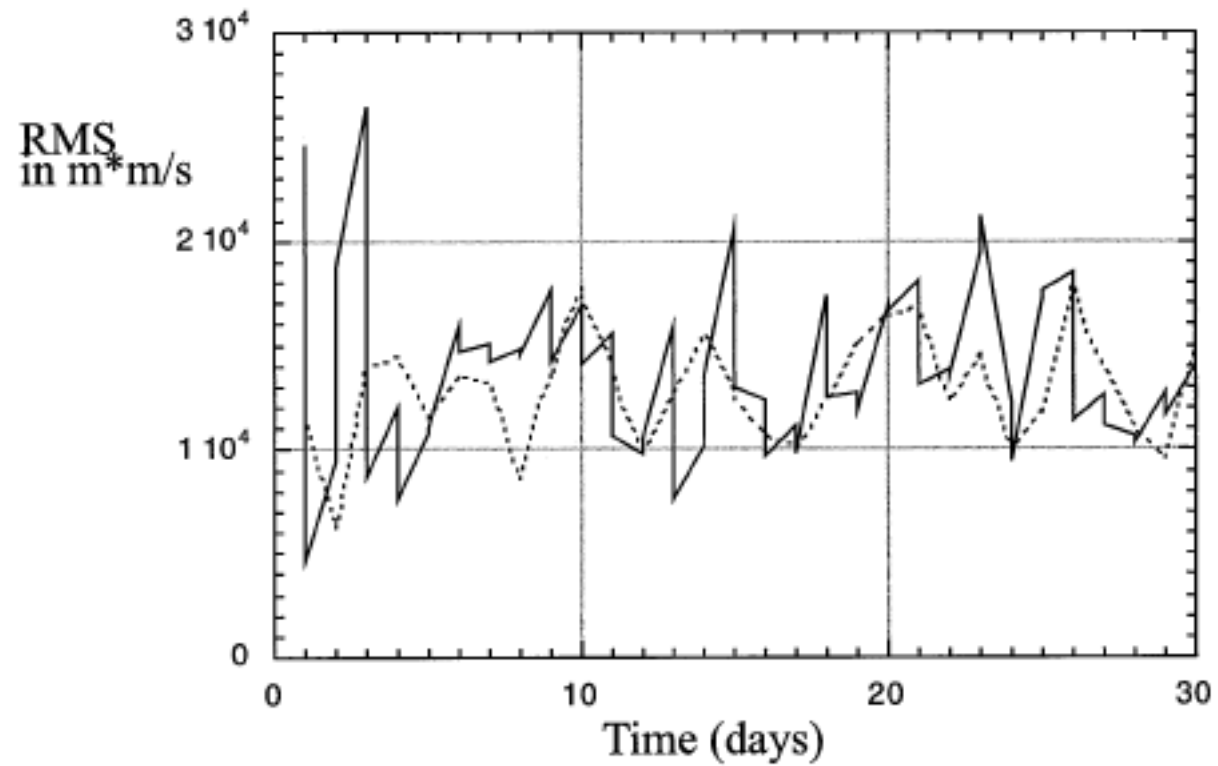
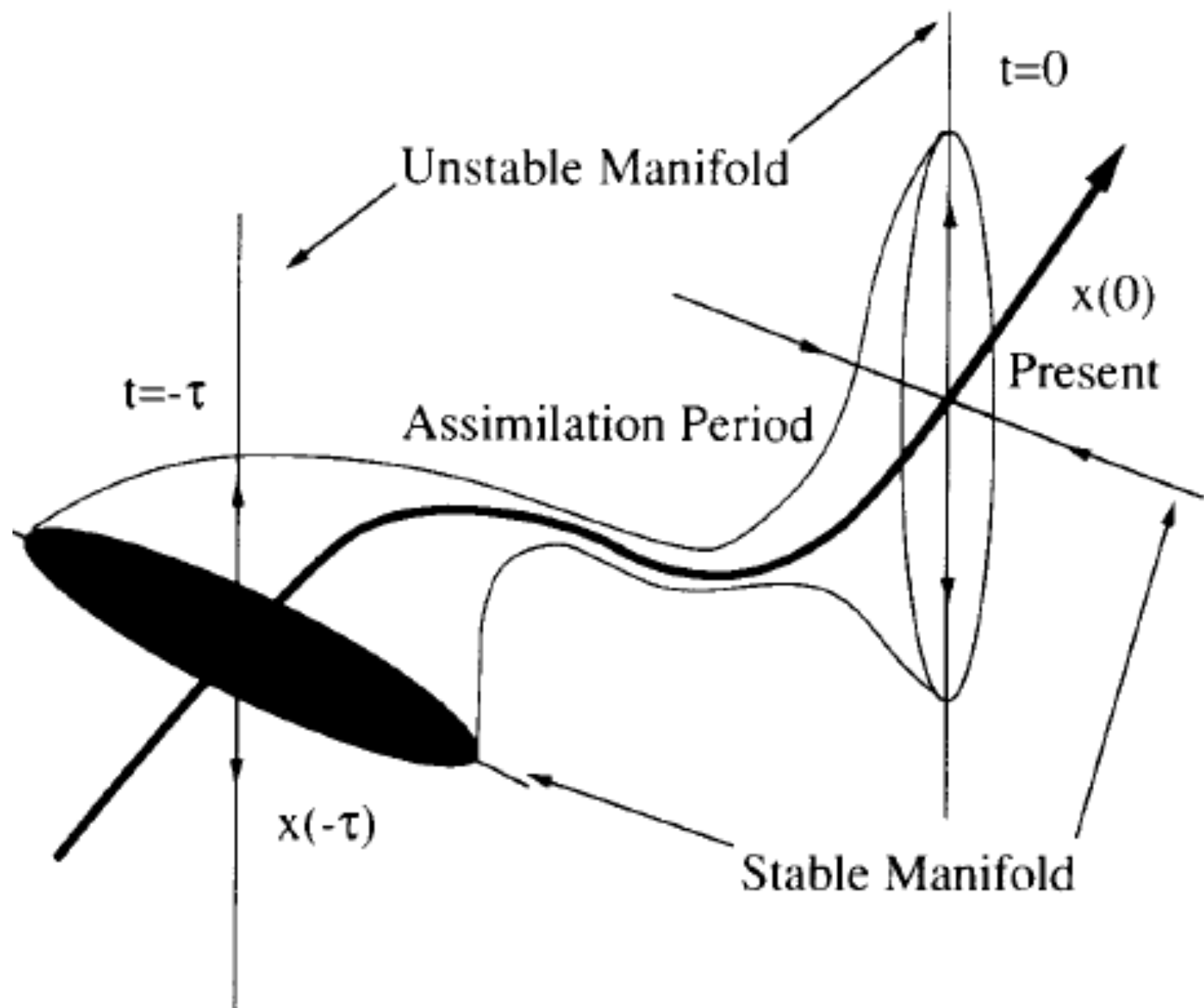


FIG. 12. Comparison of rms error ($\text{m}^2 \text{s}^{-1}$) between ensemble mean and independent observations (dotted line) and the std dev in the ensemble (solid line). The excellent agreement shows that the SIRF is working correctly.

Particle filters are actively studied (van Leeuwen, Morzfeld, ...)

If there is uncertainty on the state of the system, and dynamics of the system is perfectly known, uncertainty on the state along stable modes decreases over time, while uncertainty along unstable modes increases.

Stable (unstable) modes : perturbations to the basic state that decrease (increase) over time.



Consequence : Consider 4D-Var assimilation, which carries information both forward and backward in time, performed over time interval $[t_0, t_1]$ over uniformly distributed noisy data. If assimilating model is perfect, estimation error is concentrated in stable modes at time t_0 , and in unstable modes at time t_1 . Error is smallest somewhere within interval $[t_0, t_1]$.

Similar result holds true for Kalman filter (or more generally any form of sequential assimilation), in which estimation error is concentrated in unstable modes at any time.

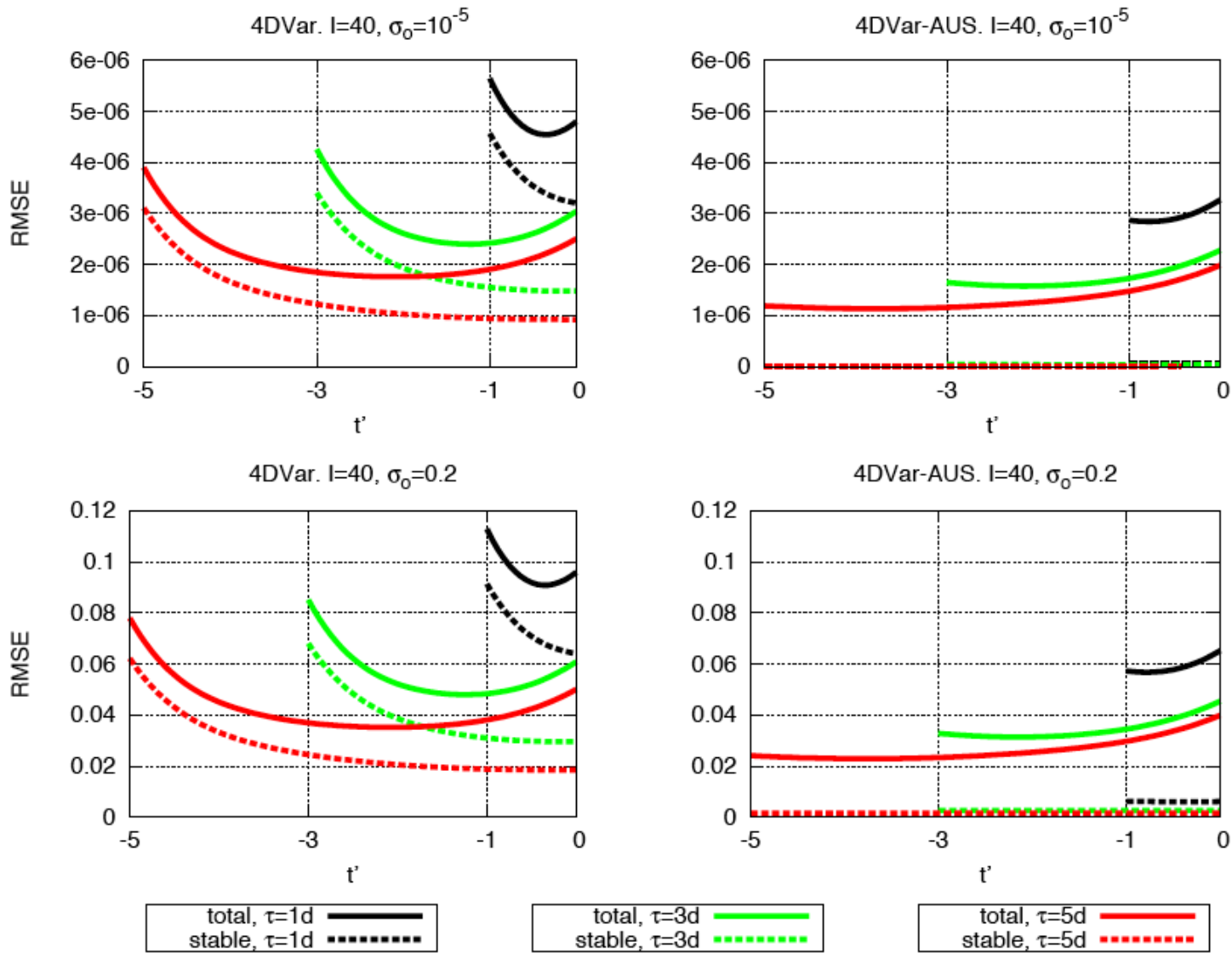


Figure 3. Time average RMS error within 1, 3, 5 days assimilation windows as a function of $t' = t - \tau$, with $\sigma_0 = .2, 10^{-5}$ for the model configuration $I = 40$. Left panel: 4DVar. Right panel: 4DVar-AUS with $N = 15$. Solid lines refer to total assimilation error, dashed lines refer to the error component in the stable subspace e_{16}, \dots, e_{40} .

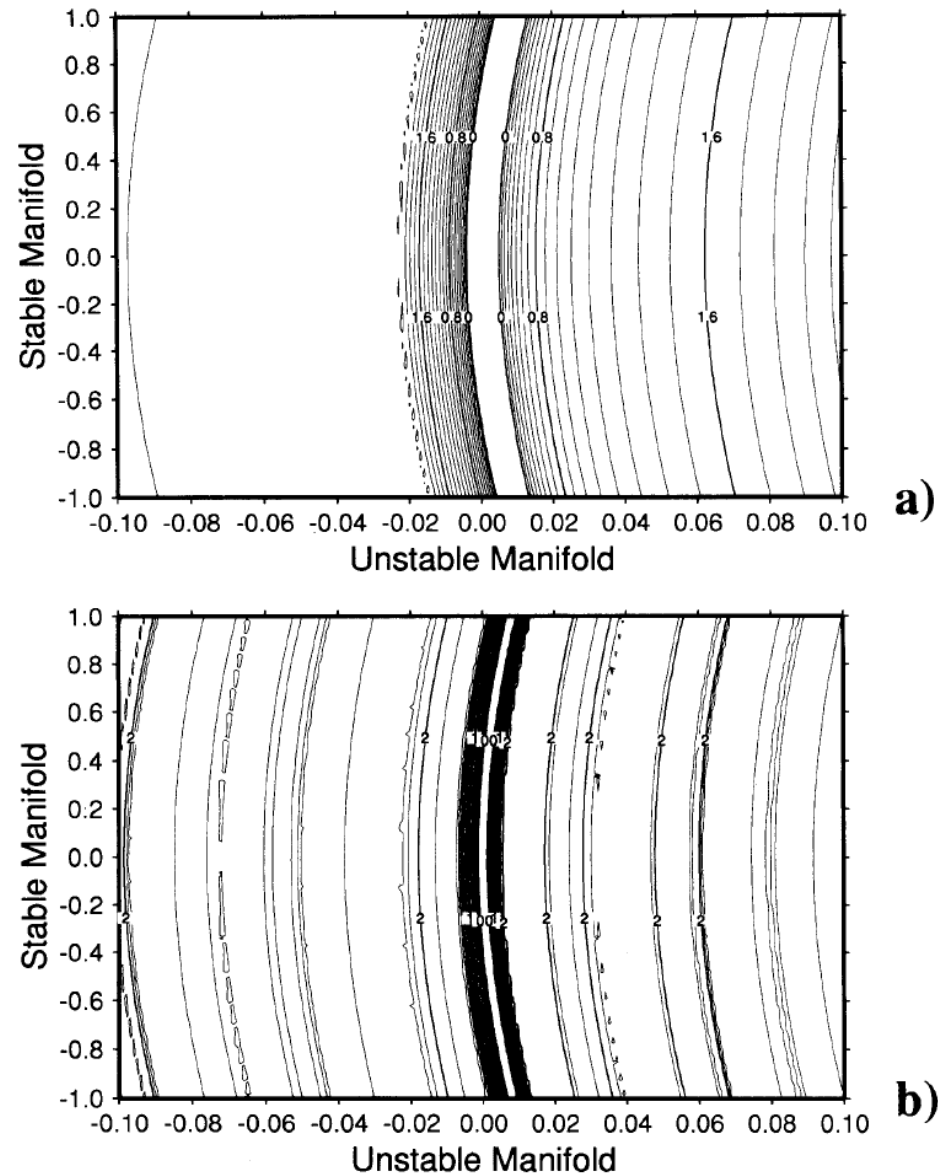


Fig. 3. Variations of the error-free forward cost-function $J'_2(\tau, \hat{x}, x)$ (Lorenz system) in the plane spanned by the stable and unstable directions, as determined from the tangent linear system (see text), and for $\tau = 6$ (panel (a)) and $\tau = 8$ (panel (b)) respectively. The metric has been distorted in order to make the stable and unstable manifolds orthogonal to each other in the figure. The scale on the contour lines is logarithmic (decimal logarithm). Contour interval: 0.1. For clarity, negative contours, which would be present only in the central “valley” directed along the stable manifold, have not been drawn.

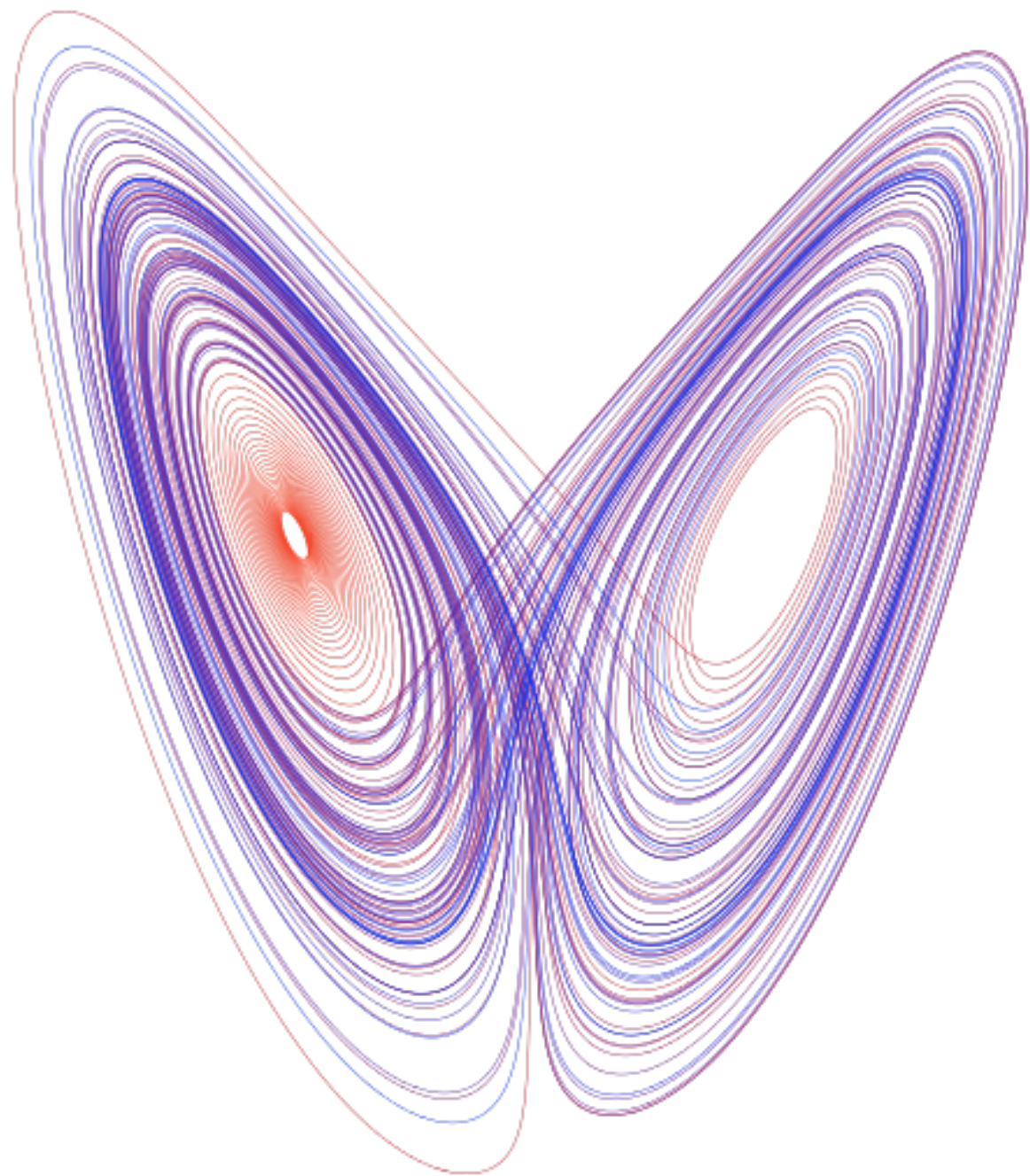
Lorenz (1963)

$$dx/dt = \sigma(y-x)$$

$$dy/dt = \rho x - y - xz$$

$$dz/dt = -\beta z + xy$$

with parameter values $\sigma = 10$, $\rho = 28$, $\beta = 8/3 \Rightarrow$ chaos



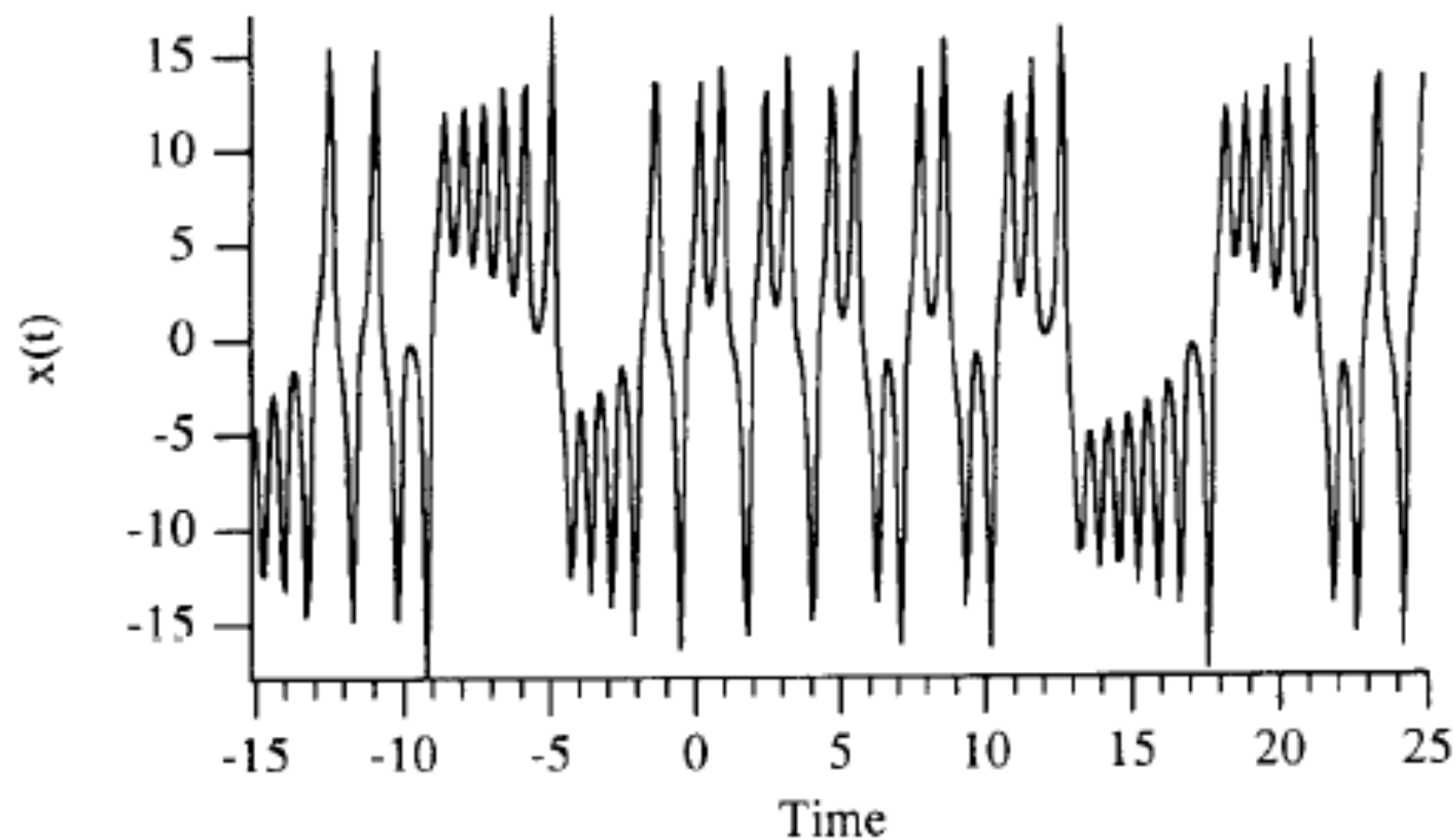


Fig. 2. Time variations, along the reference solution, of the variable $x(t)$ of the Lorenz system.

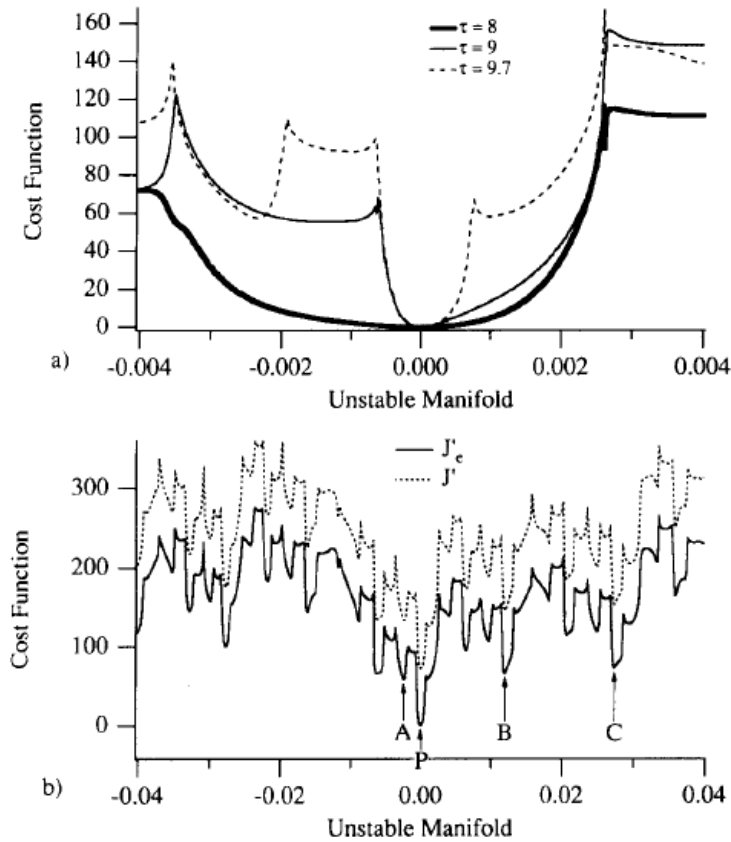


Fig. 4. Panel (a): Cross-section of the error-free forward cost-function $J'_e(\tau, \hat{x}, x)$ along the unstable manifold, for various values of τ . Panel (b). As in panel (a), for $\tau = 9.7$, and with a display interval ten times as large, respectively for the error-free forward cost-function $J'_e(\tau, \hat{x}, x)$ (solid curve) and for the error-contaminated cost-function $J_e(\tau, \hat{x}, x)$ (dashed curve). In the latter case, the total variance of the observational noise is $E^2 = 75$.

Pires *et al.*, *Tellus*, 1996 ; Lorenz system (1963)

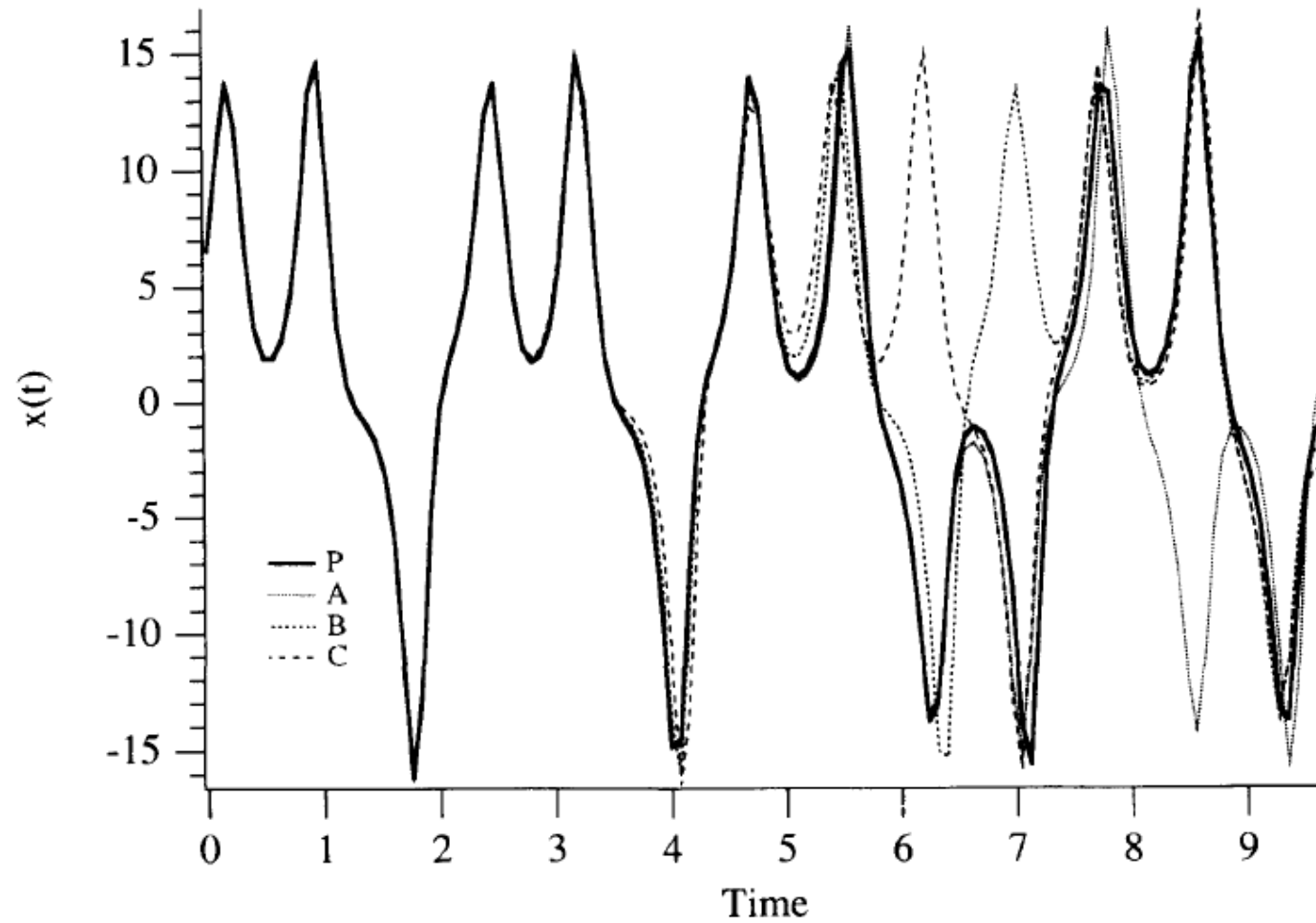


Fig. 5. Variations of the coordinate x along the orbits originating from the minima P , A , B , C (indicated in Fig. 4b) of the error-free cost-function.

Minima in the variations of objective function correspond to solutions that have bifurcated from the observed solution, and to different folds in state space.

Quasi-Static Variational Assimilation (QSVA). Increase progressively length of the assimilation window, starting each new assimilation from the result of the previous one. This should ensure, at least if observations are in a sense sufficiently dense in time, that current estimation of the system always lies in the attractive basin of the absolute minimum of objective function (Pires *et al.*, Swanson *et al.*, Luong, Järvinen *et al.*)

.

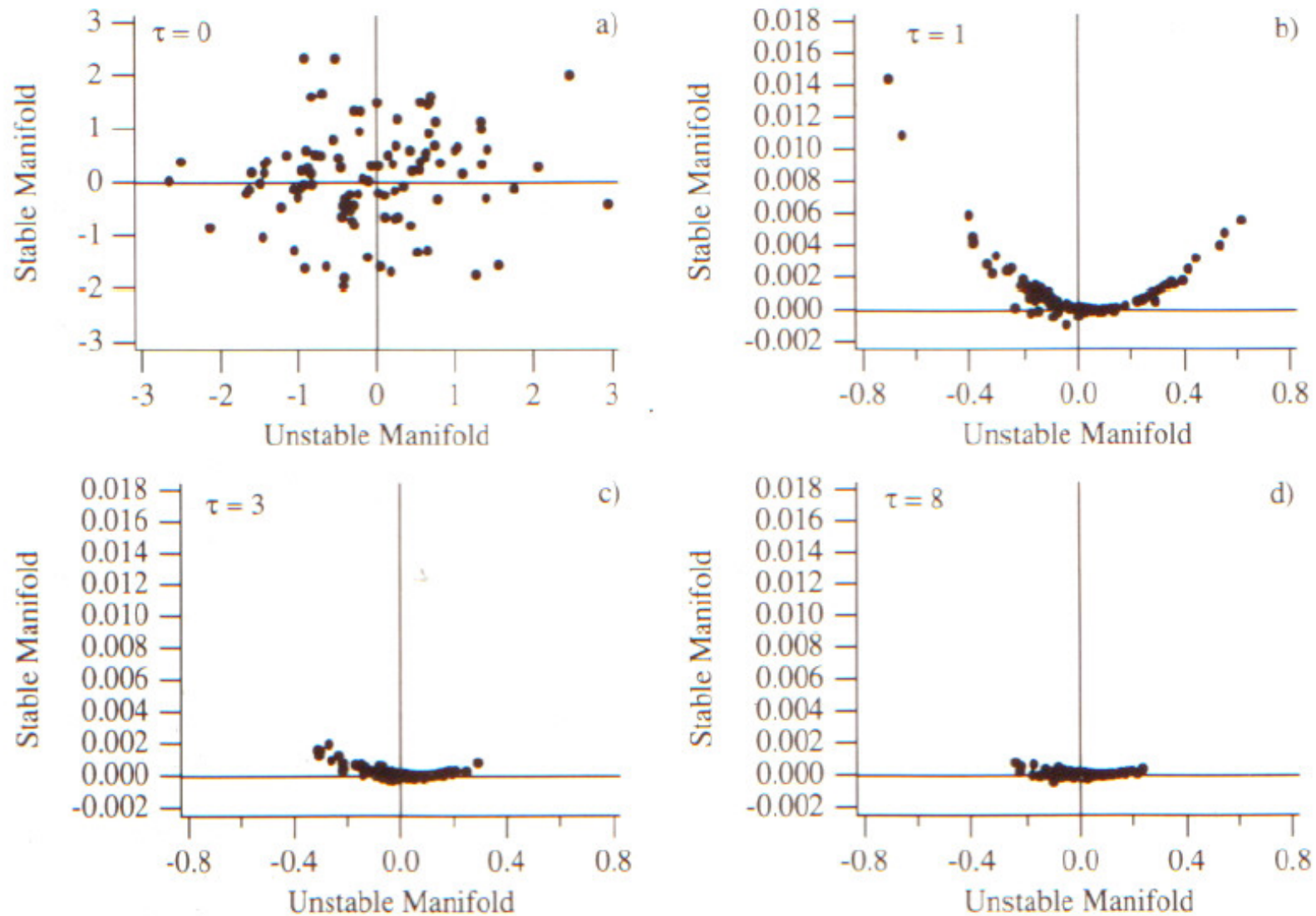


Fig. 7. Projection of the 100 minimizing solutions, at the end of the assimilation period, onto the plane spanned by the stable and unstable directions, defined as in Fig. 3. Values of τ are indicated on the panels. The projection is not an orthogonal projection, but a projection parallel to the local velocity vector $(dx/dt, dy/dt, dz/dt)$ (central manifold).

$\mu(C(\tau, x))$	Cloud of points QSVA	Cloud of points raw assimilation	Linear tangent system	Upper bound
$\tau = 0$	1	1	1	1
$\tau = 1$	0.36	0.37	0.39	0.46
$\tau = 2$	5.9×10^{-2}	5.74	4.5×10^{-2}	0.401
$\tau = 3$	3.3×10^{-2}	29.4	2.9×10^{-2}	0.397
$\tau = 8$	1.4×10^{-2}	59.9	*	0.396

In the left column, the estimates are calculated from the ensemble of 100 assimilations (see also Fig. 7). The 2nd column contains the values obtained from the raw assimilation. In the 3rd column, the estimates are obtained from the tangent linear system and eqs. (3.5–3.9) (the star indicates a computational overflow). The estimates in the right-hand column are the upper bounds defined by eq. (3.13).

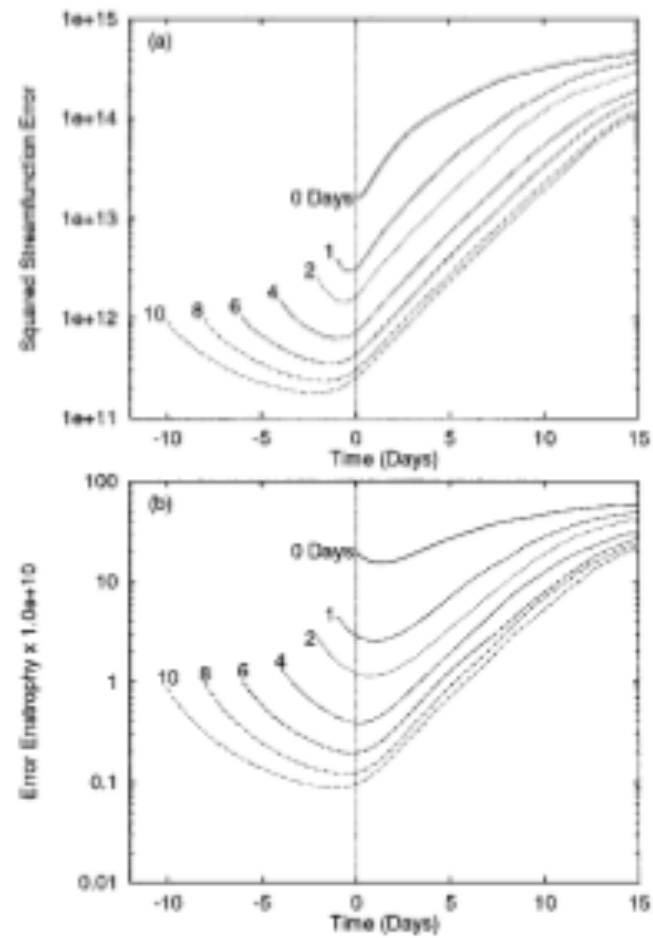


Fig. 5. Median values of the (a) streamfunction squared error, and (b) enstrophy error for the 200 forecast set as a function of forecast time and of the assimilation time T_a .

Swanson, Vautard and Pires, 1998, *Tellus*, **50A**, 369-390

Since, after an assimilation has been performed over a period of time, uncertainty is likely to be concentrated in modes that have been unstable, it might be useful for the next assimilation, and at least in terms of cost efficiency, to concentrate corrections on the background in those modes.

Actually, presence of residual noise in stable modes can be damageable for analysis and subsequent forecast.

Assimilation in the Unstable Subspace (AUS) (Carrassi *et al.*, 2007, 2008, for the case of 3D-Var)

Four-dimensional variational assimilation in the unstable subspace
(4DVar-AUS)

Trevisan *et al.*, 2010, Four-dimensional variational assimilation in the unstable subspace and the optimal subspace dimension, *Q. J. R. Meteorol. Soc.*, **136**, 487-496.

4D-Var-AUS

Algorithmic implementation

Define N perturbations to the current state, and evolve them according to the tangent linear model, with periodic reorthonormalization in order to avoid collapse onto the dominant Lyapunov vector (same algorithm as for computation of Lyapunov exponents).

Cycle successive 4D-Var's, restricting at each cycle the modification to be made on the current state to the space spanned by the N perturbations emanating from the previous cycle (if N is the dimension of state space, that is identical with standard 4D-Var).

Experiments performed on the Lorenz (1996) model

$$\frac{d}{dt}x_j = (x_{j+1} - x_{j-2})x_{j-1} - x_j + F$$

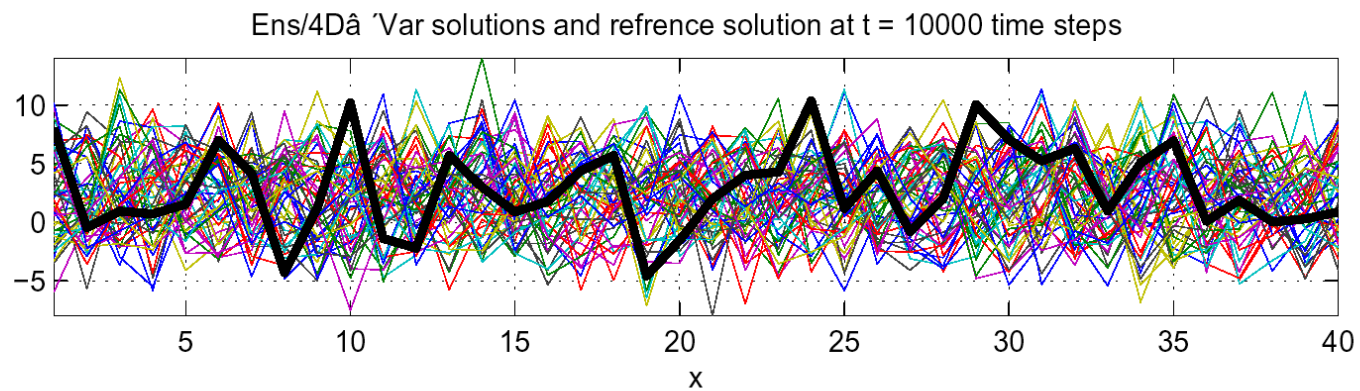
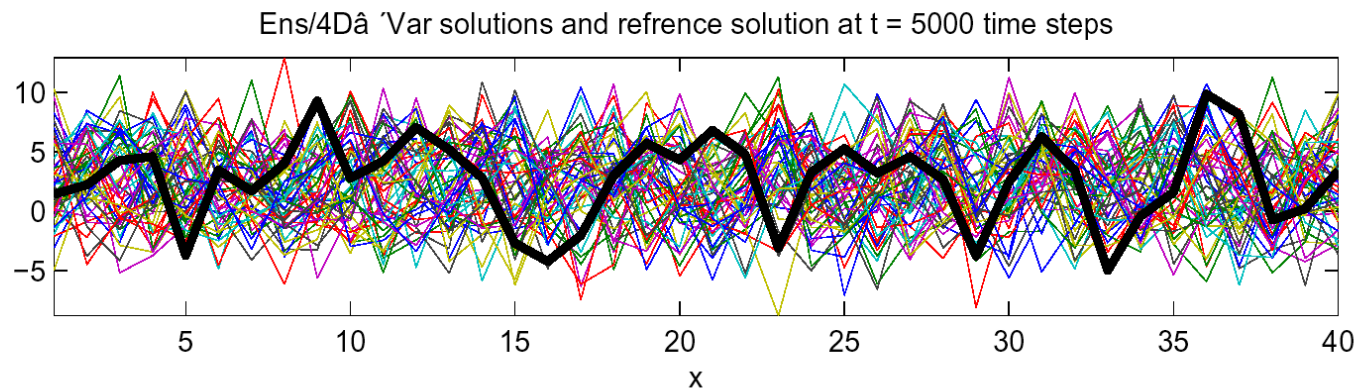
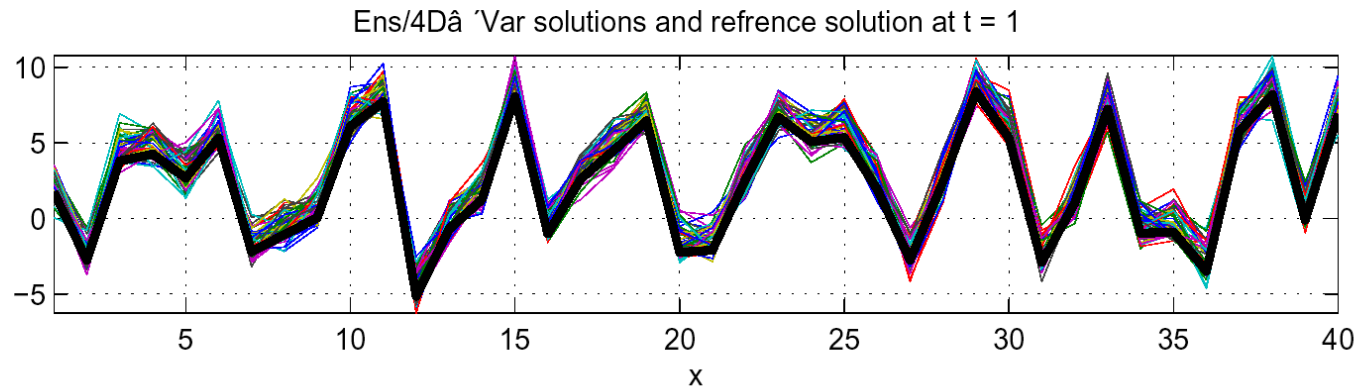
with $j = 1, \dots, I$.

with value $F = 8$, which gives rise to chaos.

Three values of I have been used, namely $I = 40, 60, 80$, which correspond to respectively $N^+ = 13, 19$ and 26 positive Lyapunov exponents.

In all three cases, the largest Lyapunov exponent corresponds to a doubling time of about 2 days (with 1 'day' = 1/5 model time unit).

Identical twin experiments (perfect model)



Lorenz'96 model (M. Jardak)

‘Observing system’ defined as in Fertig *et al.* (*Tellus*, 2007):

At each observation time, one observation every four grid points (observation points shifted by one grid point at each observation time).

Observation frequency : 1.5 hour

Random gaussian observation errors with expectation 0 and standard deviation $\sigma_0 = 0.2$ (‘climatological’ standard deviation 5.1).

Sequences of variational assimilations have been cycled over windows with length $\tau = 1, \dots, 5$ days. Results are averaged over 5000 successive windows.

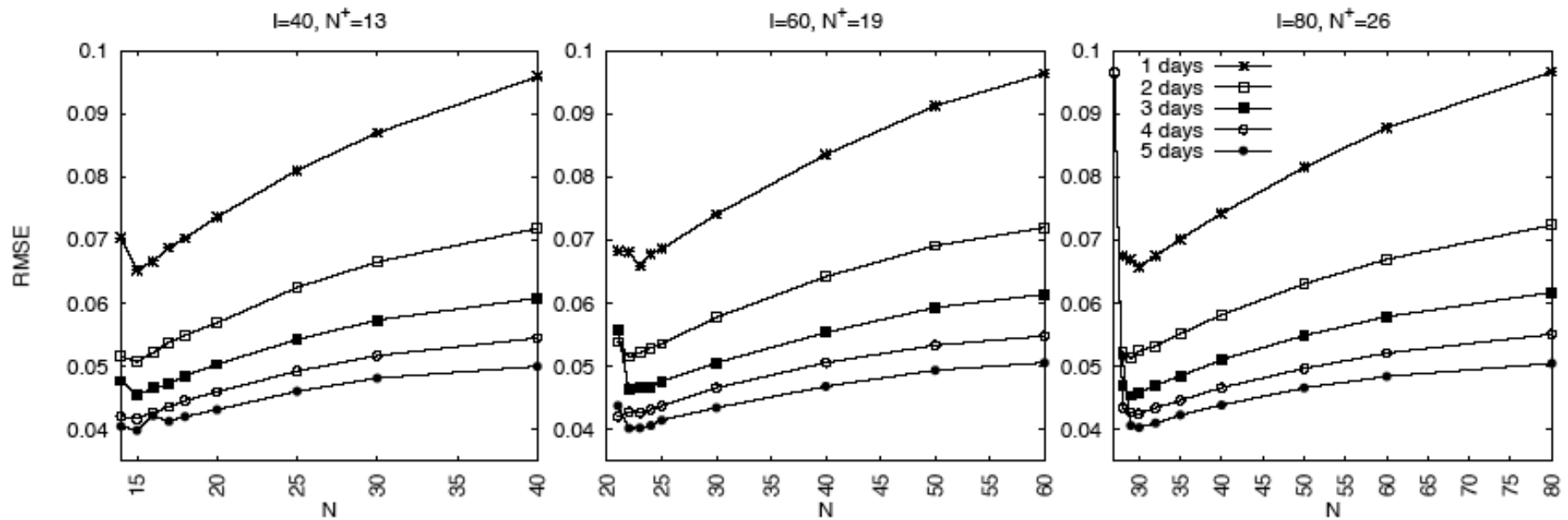


Figure 1. Time average RMS analysis error at $t = \tau$ as a function of the subspace dimension N for three model configurations: $I=40, 60, 80$. Different curves in the same panel refer to different assimilation windows from 1 to 5 days. The observation error standard deviation is $\sigma_o = 0.2$.

No explicit background term (*i. e.*, with error covariance matrix) in objective function : information from past lies in the background to be updated, and in the N perturbations which define the subspace in which updating is to be made.

Best performance for N slightly above number N^+ of positive Lyapunov exponents.

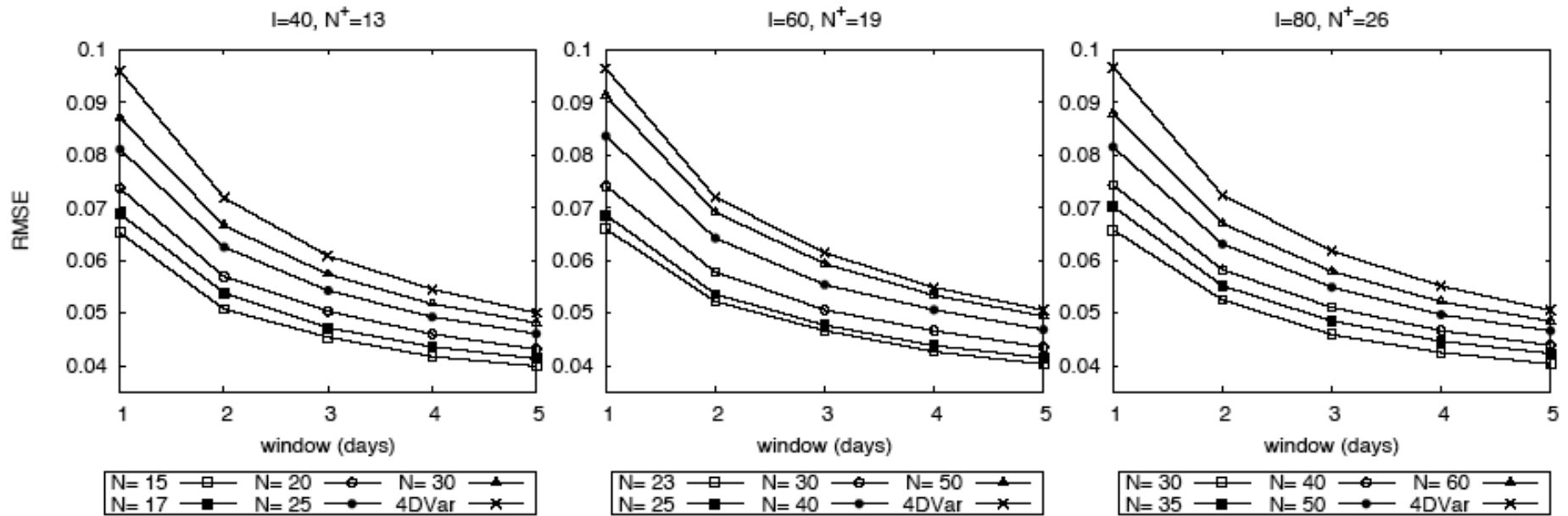


Figure 2. Time average RMS analysis error at $t = \tau$ as a function of the length of the assimilation window for three model configurations: $I=40, 60, 80$. Different curves in the same panel refer to a different subspace dimension N of 4DVar-AUS and to standard 4DVar. $\sigma_o = 0.2$.

Different curves are almost identical on all three panels. Relative improvement obtained by decreasing subspace dimension N to its optimal value is largest for smaller window length τ .

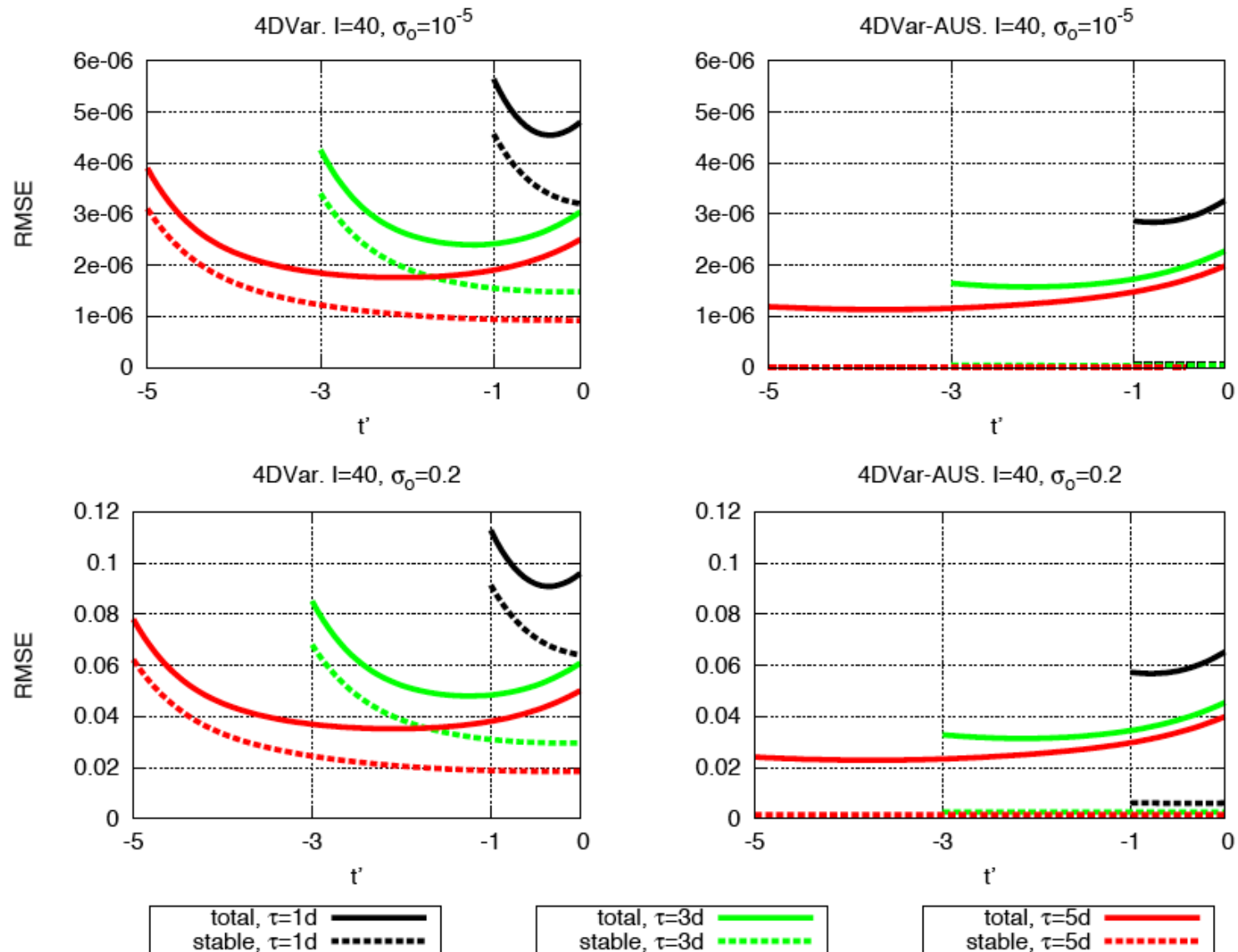


Figure 3. Time average RMS error within 1, 3, 5 days assimilation windows as a function of $t' = t - \tau$, with $\sigma_0 = .2, 10^{-5}$ for the model configuration $I = 40$. Left panel: 4DVar. Right panel: 4DVar-AUS with $N = 15$. Solid lines refer to total assimilation error, dashed lines refer to the error component in the stable subspace e_{16}, \dots, e_{40} .

Experiments have been performed in which an explicit background term was present, the associated error covariance matrix having been obtained as the average of a sequence of full **4D-Var**'s.

The estimates are systematically improved, and more for full **4D-Var** than for **4D-Var-AUS**. But they remain qualitatively similar, with best performance for **4D-Var-AUS** with N slightly above N^+ .

Minimum of objective function cannot be made smaller by reducing control space. Numerical tests show that minimum of objective function is smaller (by a few percent) for full **4D-Var** than for **4D-Var-AUS**. Full **4D-Var** is closer to the noisy observations, but farther away from the truth. And tests also show that full **4D-Var** performs best when observations are perfect (no noise).

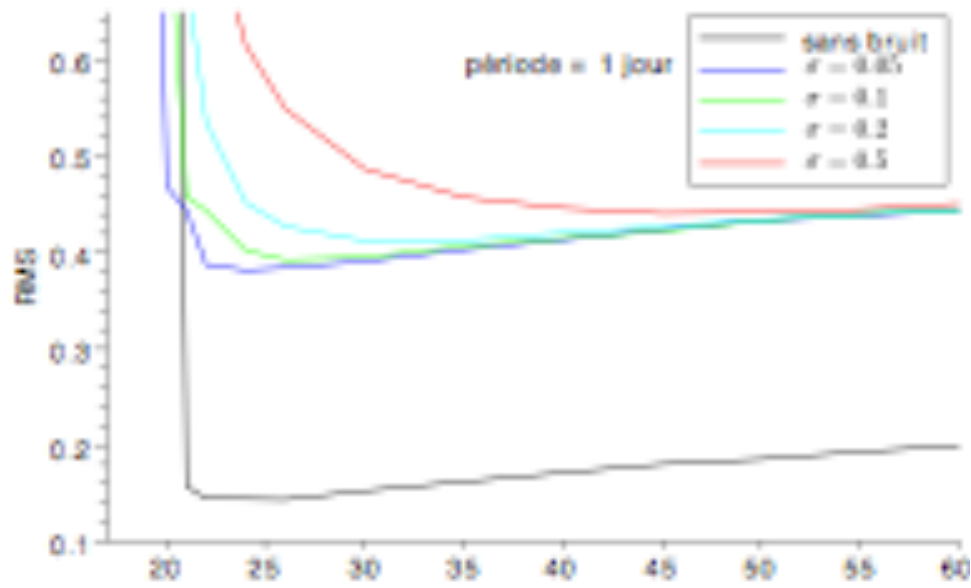
Results show that, if all degrees of freedom that are available to the model are used, the minimization process introduces components along the stable modes of the system, in which no error is present, in order to ensure a closer fit to the observations. This degrades the closeness of the fit to reality. The optimal choice is to restrict the assimilation to the unstable modes.

Can have major practical algorithmic implications.

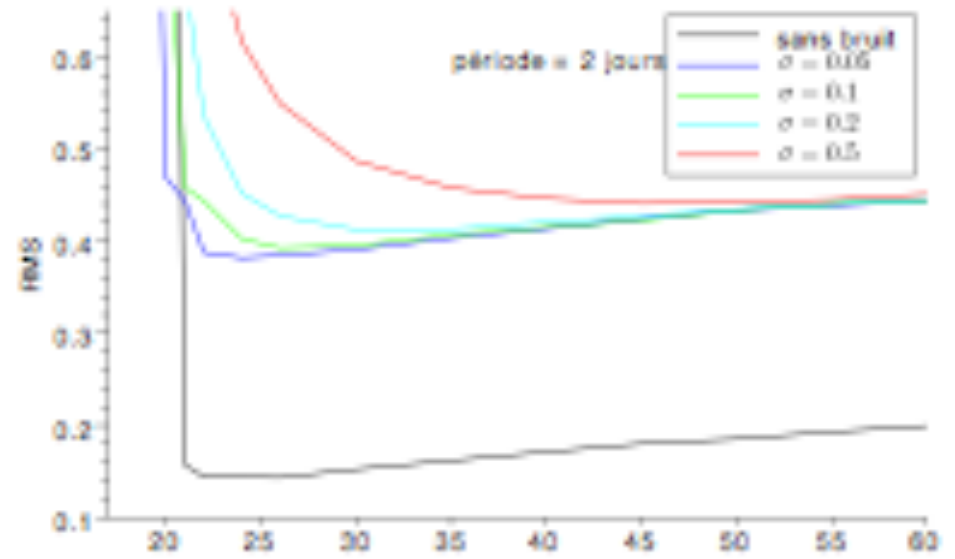
Questions.

- Degree of generality of results ?

- Impact of model errors ?



$\tau = 1$ day



$\tau = 2$ days

Time averaged rms analysis error at the end of the assimilation window (with length τ) as a function of increment subspace dimension ($I = 60, N^+ = 19$), for different amplitudes of white model noise.

(W. Ohayon and O. Pannekoucke, 2011).

Conclusions

Error concentrates in unstable modes at the end of assimilation window. It must therefore be sufficient, at the beginning of new assimilation cycle, to introduce increments only in the subspace spanned by those unstable modes.

In the perfect model case, assimilation is most efficient when increments are introduced in a space with dimension slightly above the number of non-negative Lyapunov exponents.

In the case of imperfect model (and of strong constraint assimilation), preliminary results lead to similar conclusions, with larger optimal subspace dimension, and less well marked optimality. Further work necessary.

In agreement with theoretical and experimental results obtained for Kalman Filter assimilation (Trevisan and Palatella, McLaughlin).

Ensemble Variational Assimilation and Bayesian Estimation

Olivier Talagrand¹ and Mohamed Jardak^{1,2}

1. Laboratoire de Météorologie Dynamique/IPSL

École Normale Supérieure, Paris, France

2. Meteorological Office, Exeter, UK

Workshop

*Theoretical aspects of ensemble data assimilation
for the Earth system*

Les Houches, France

6 April 2015

Assimilation considered as a problem in bayesian estimation.

Determine the conditional probability distribution for the state of the system, knowing everything we know (the *data*), viz.,

- observations proper
- physical laws governing the system ('*model*')
- ...

Jaynes, E. T., 2003, *Probability theory: the logic of science*, Cambridge University Press

Tarantola, A., 2005, *Inverse Problem Theory and Methods for Model Parameter Estimation*, Society for Industrial and Applied Mathematics (<http://www.ipgp.jussieu.fr/~tarantola/Files/Professional/Books/InverseProblemTheory.pdf>)

Data of the form

$$z = \Gamma x + \zeta, \quad \zeta \sim \mathcal{N}[\mu, S]$$

Known data vector z belongs to *data space* \mathcal{D} , $\dim \mathcal{D} = m$,

Unknown state vector x belongs to *state space* \mathcal{X} , $\dim \mathcal{X} = n$

Γ known ($m \times n$)-matrix, ζ unknown 'error'

Then conditional probability distribution is

$$P(x | z) = \mathcal{N}[x^a, P^a]$$

where

$$x^a = (\Gamma^T S^{-1} \Gamma)^{-1} \Gamma^T S^{-1} [z - \mu]$$

$$P^a = (\Gamma^T S^{-1} \Gamma)^{-1}$$

Determinacy condition : $\text{rank} \Gamma = n$. Requires $m \geq n$.

Variational form.

Conditional expectation x^a minimizes following scalar *objective function*, defined on state space \mathcal{X}

$$\xi \in \mathcal{X} \rightarrow \mathcal{J}(\xi) \equiv (1/2) [\Gamma\xi - (z-\mu)]^T S^{-1} [\Gamma\xi - (z-\mu)]$$

Variational assimilation, implemented heuristically in many places on (not too) nonlinear data operators Γ .

$$P^a = [\partial^2 \mathcal{J} / \partial \xi^2]^{-1}$$

Conditional probability distribution

$$P(x | z) = \mathcal{N}[x^a, P^a]$$

with

$$x^a = (\Gamma^T S^{-1} \Gamma)^{-1} \Gamma^T S^{-1} [z - \mu]$$

$$P^a = (\Gamma^T S^{-1} \Gamma)^{-1}$$

Ready recipe for determining Monte-Carlo sample of conditional pdf $P(x | z)$:

- Perturb data vector z according to its own error probability distribution

$$z \rightarrow z' = z + \delta, \quad \delta \sim \mathcal{N}[0, S]$$

and compute

$$x'^a = (\Gamma^T S^{-1} \Gamma)^{-1} \Gamma^T S^{-1} [z' - \mu]$$

x'^a is distributed according to $\mathcal{N}[x^a, P^a]$

Ensemble Variational Assimilation (EnsVar) implements that algorithm, the expectations x'^a being computed by standard variational assimilation (optimization)

Purpose of the present work

- Objectively evaluate EnsVar as a probabilistic estimator in nonlinear and/or non-Gaussian cases.
- Objectively compare with other existing ensemble assimilation algorithms : *Ensemble Kalman Filter (EnKF)*, *Particle Filters (PF)*
- Simulations performed on two small-dimensional chaotic systems, the Lorenz'96 model and the Kuramoto-Sivashinsky equation

Purely heuristic !

Conclusion. Works very well, at least on small dimension chaotic systems, and using *Quasi-Static Variational Assimilation (QSVA)* over long assimilation periods

Experimental procedure (1)

0. Define a *reference solution* x_t^r by integration of the numerical model

1. Produce ‘observations’ at successive times t_k of the form

$$y_k = H_k x_k + \varepsilon_k$$

where H_k is (usually, but not necessarily) the unit operator, and ε_k is a random (usually, but not necessarily, Gaussian) ‘observation error’.

Experimental procedure (2)

2. For given observations y_k , repeat N_{ens} times the following process

- ‘Perturb’ the observations y_k as follows

$$y_k \rightarrow z_k = y_k + \delta_k$$

where δ_k is an independent realization of the probability distribution which has produced ε_k .

- Assimilate the ‘perturbed’ observations z_k by variational assimilation

This produces N_{ens} (=30) model solutions over the assimilation window, considered as making up a tentative sample of the conditional probability distribution for the state of the observed system over the assimilation window.

The process 1-2 is then repeated over N_{real} successive assimilation windows. Validation is performed on the set of N_{real} (=9000) ensemble assimilations thus obtained.

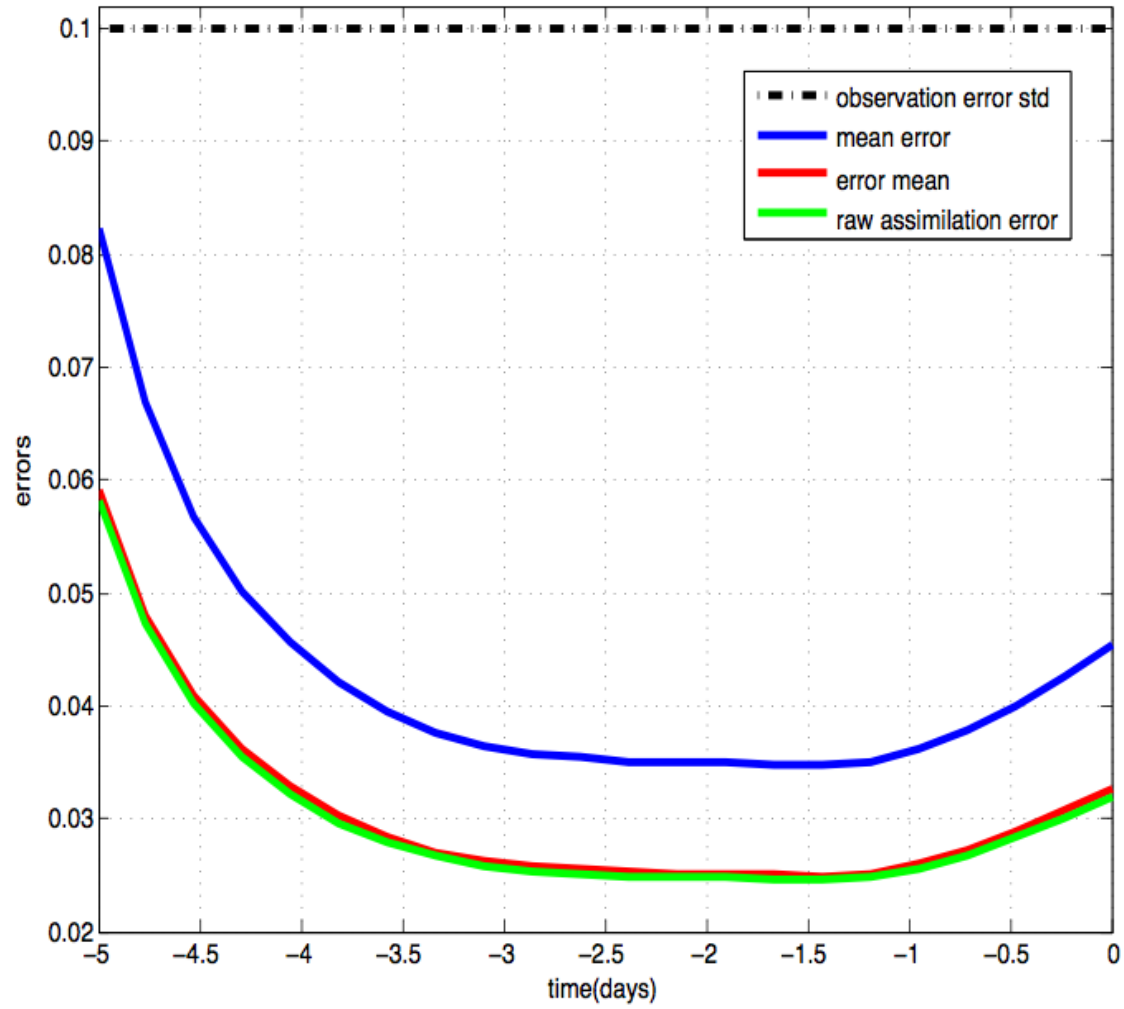
The Lorenz96 model

- Forward model

$$\frac{dx_k}{dt} = (x_{k+1} - x_{k-2})x_{k-1} - x_k + F \quad \text{for } k = 1, \dots, N$$

- Set-up parameters :

- ① the index k is cyclic so that $x_{k-N} = x_{k+N} = x_k$.
- ② $F = 8$, external driving force.
- ③ $-x_k$, a damping term.
- ④ $N = 40$, the system size.
- ⑤ $N_{ens} = 30$, number of ensemble members.
- ⑥ $\frac{1}{\lambda_{max}} \simeq 2.5days$, λ_{max} the largest Lyapunov exponent.
- ⑦ $\Delta t = 0.05 = 6hours$, the time step.
- ⑧ frequency of observations : every 12 hours.
- ⑨ number of realizations : 9000 realizations.



Linearized Lorenz'96. 5 days

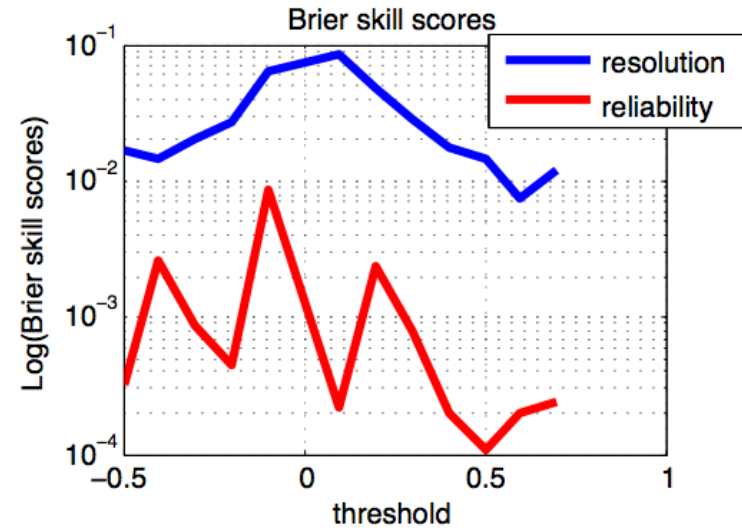
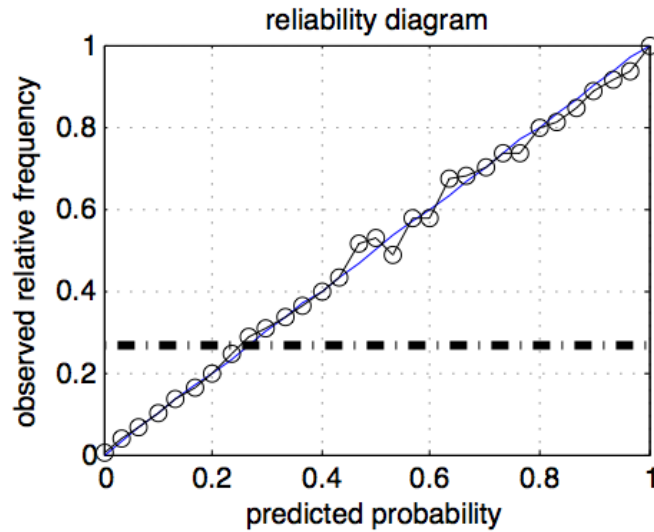
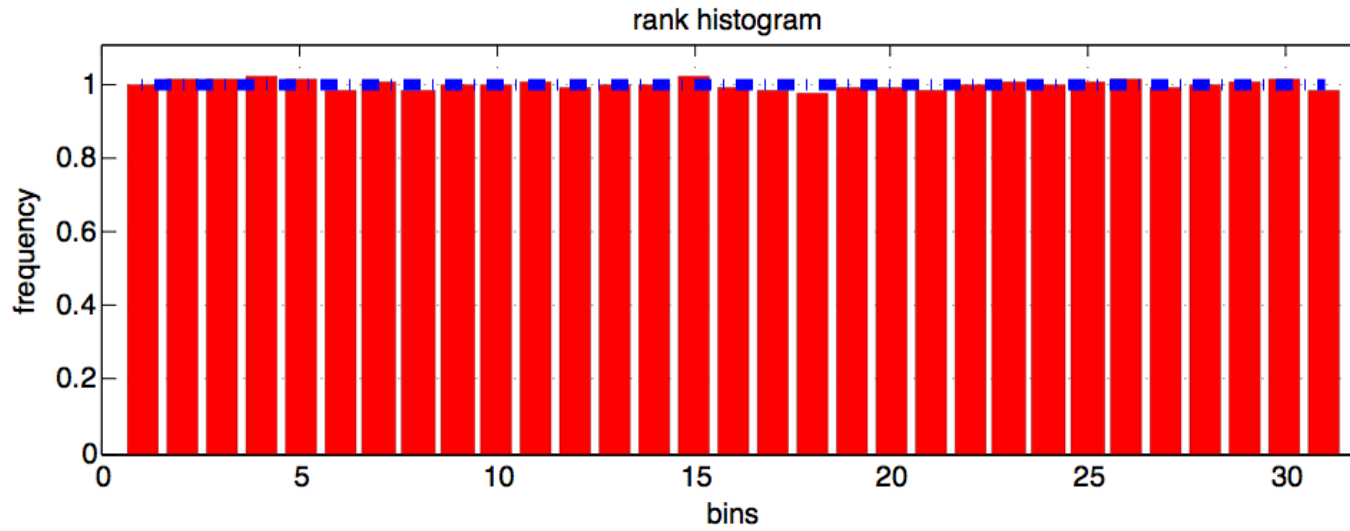
How to objectively evaluate the performance of an ensemble (or more generally probabilistic) estimation system ?

- There is no general objective criterion for Bayesianity
- We use instead the weaker property of *reliability*, *i. e.* statistical consistency between predicted probabilities and observed frequencies of occurrence (it rains with frequency 40% in the circumstances where I have predicted 40% probability for rain).

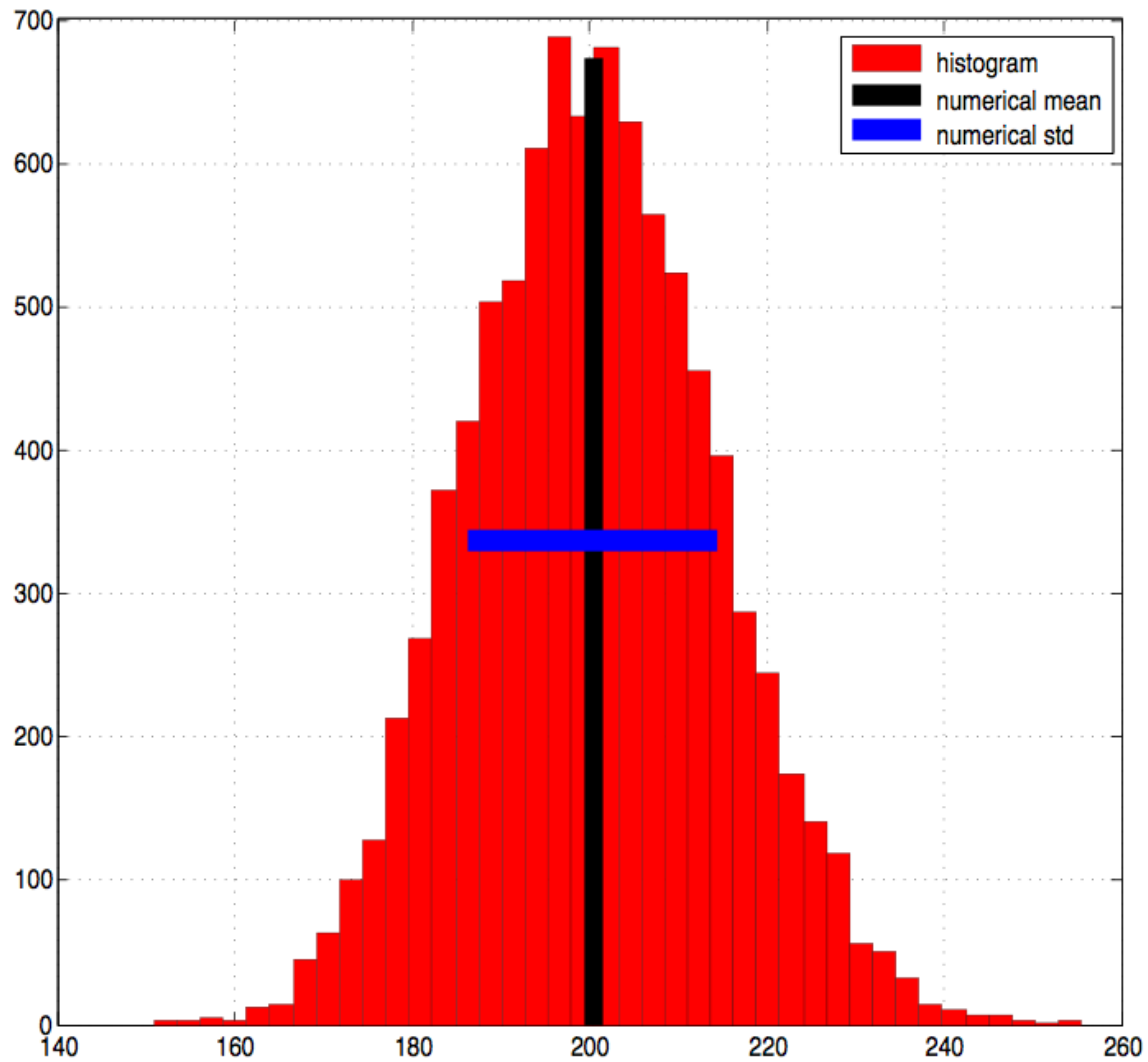
Reliability can be objectively validated, provided a large enough sample of realizations of the estimation system is available.

Bayesianity implies reliability, the converse not being true.

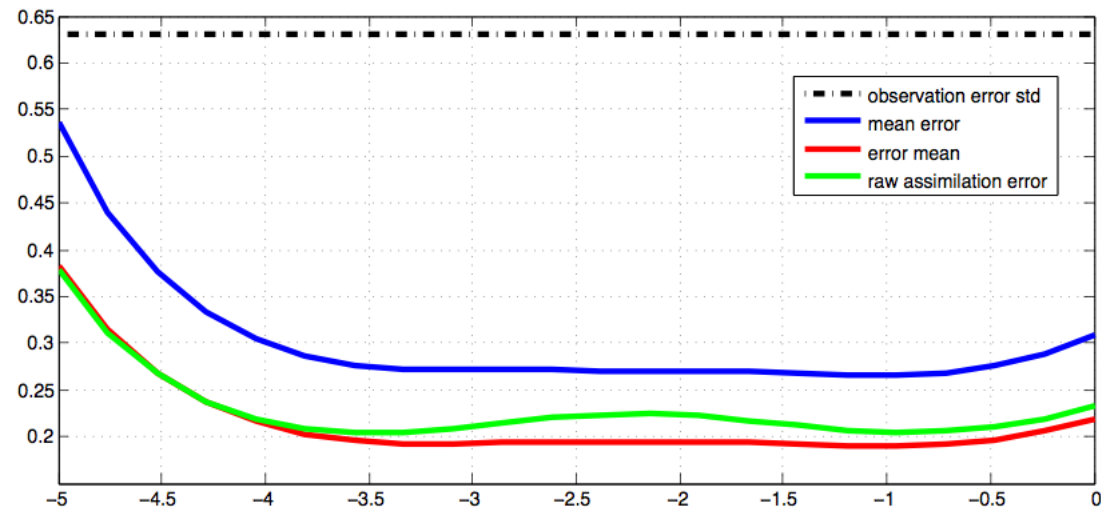
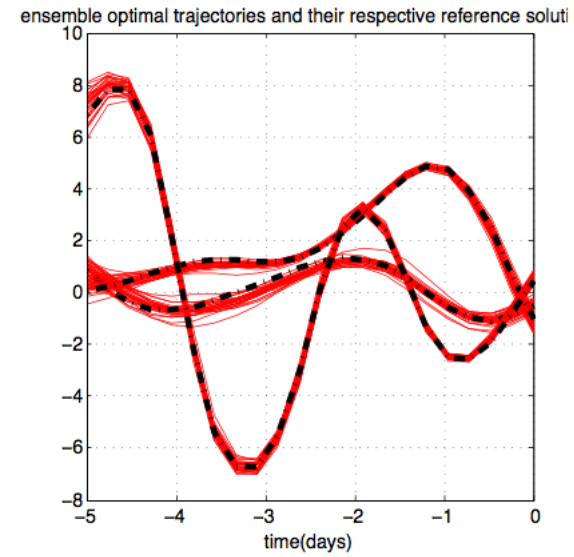
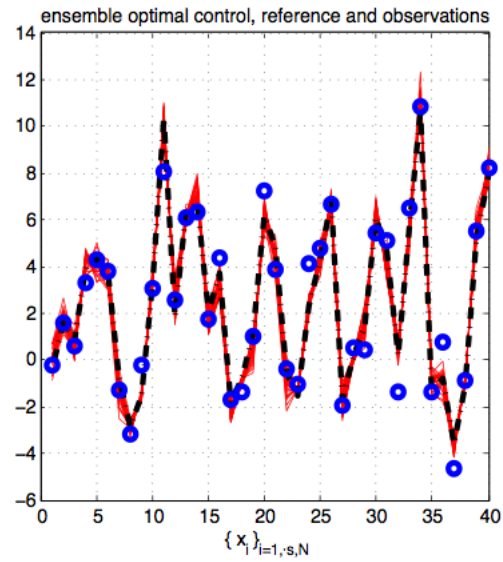
- We also evaluate *resolution*, which bears no direct relation to bayesianity, and is best defined as the degree of statistical dependence between the predicted probability distribution and the verifying observation (J. Bröcker). Resolution, beyond reliability, measures the degree of practical accuracy of the ensembles.



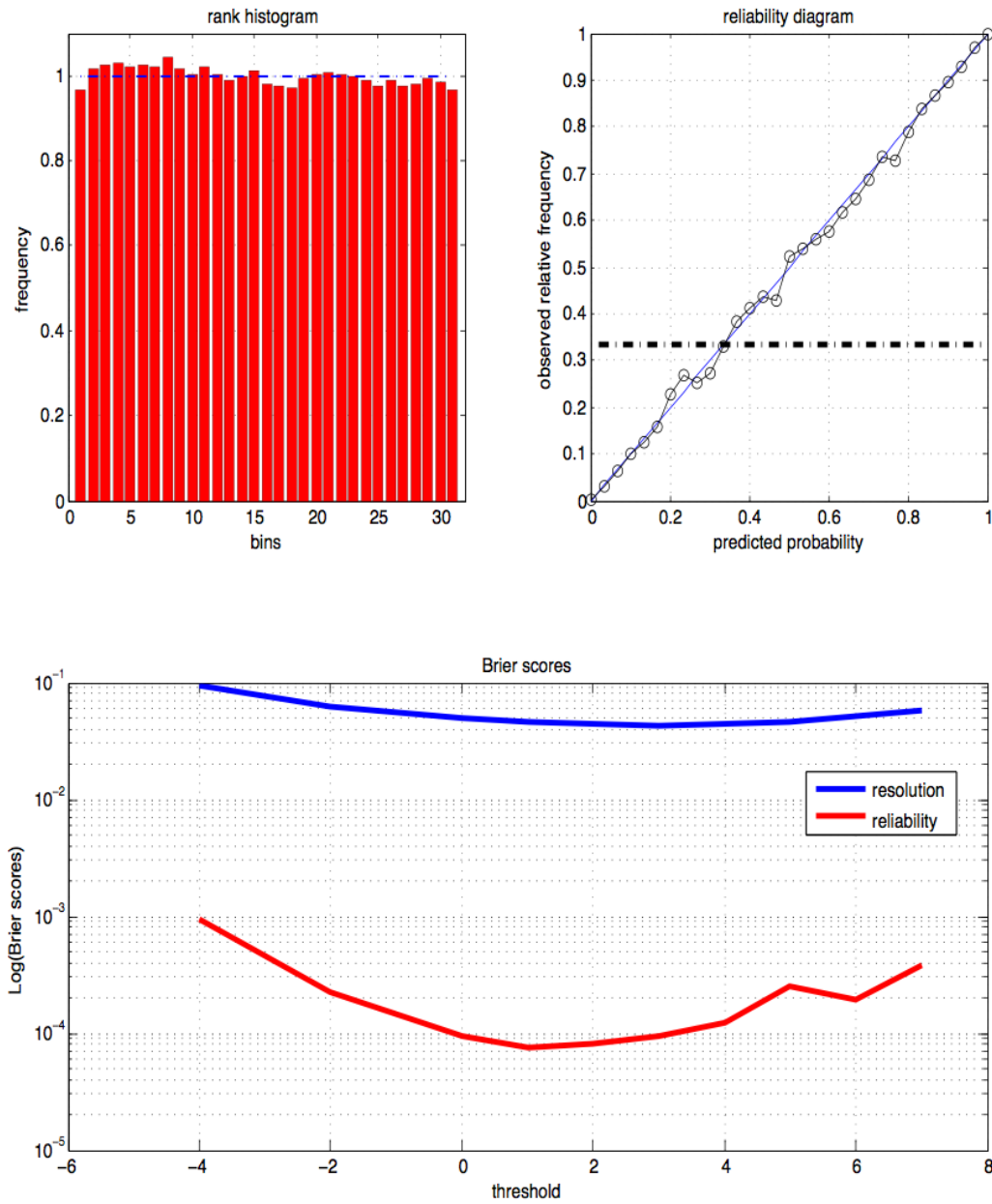
Linearized Lorenz'96. 5 days



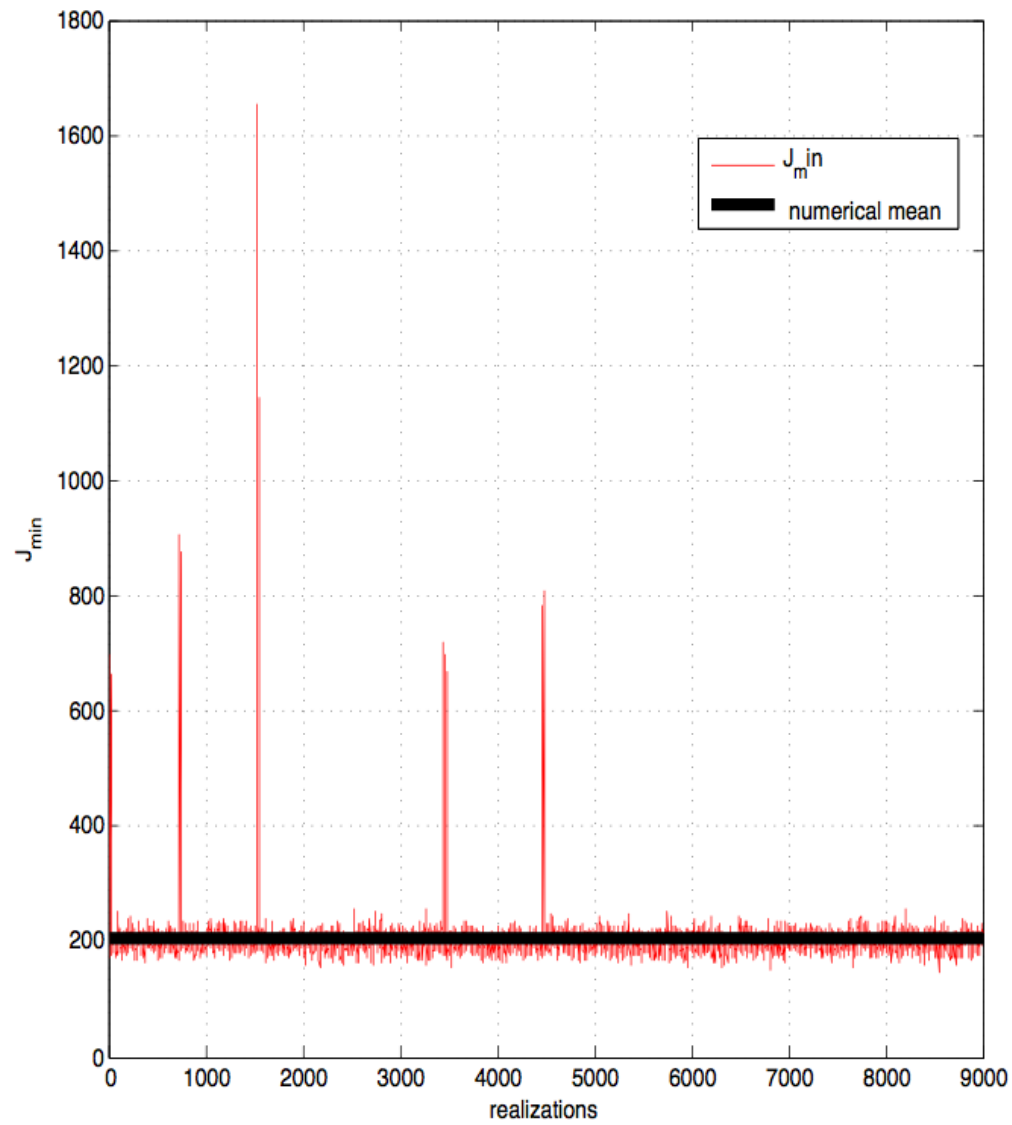
Linearized Lorenz'96. 5 days. Histogram of \mathcal{J}_{min}
 $E(\mathcal{J}_{min}) = p/2 (=200)$; $\sigma(\mathcal{J}_{min}) = \sqrt{(p/2)} (\approx 14.14)$



Nonlinear Lorenz'96. 5 days

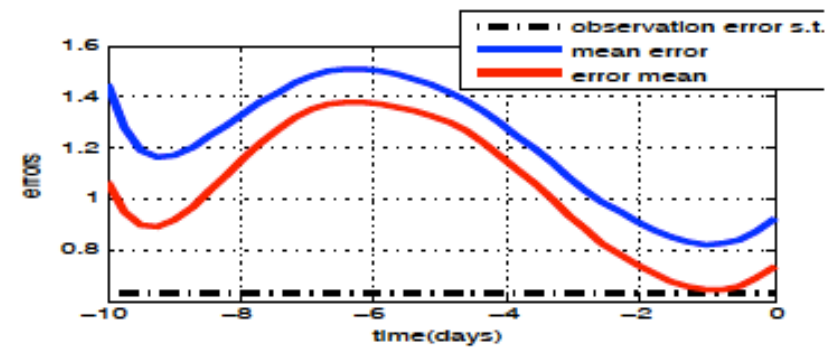
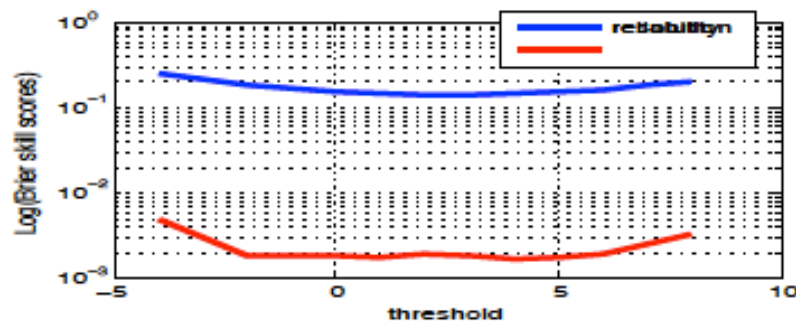
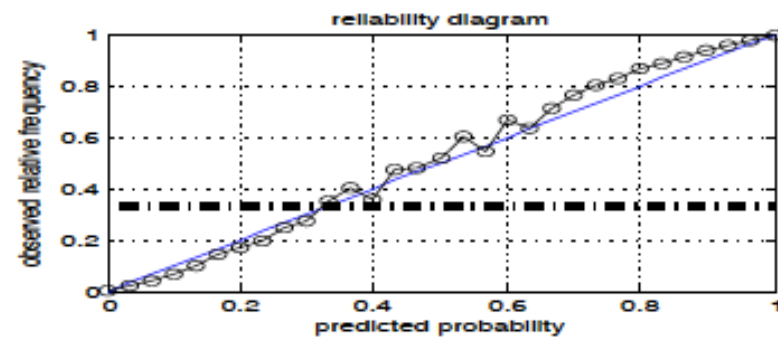
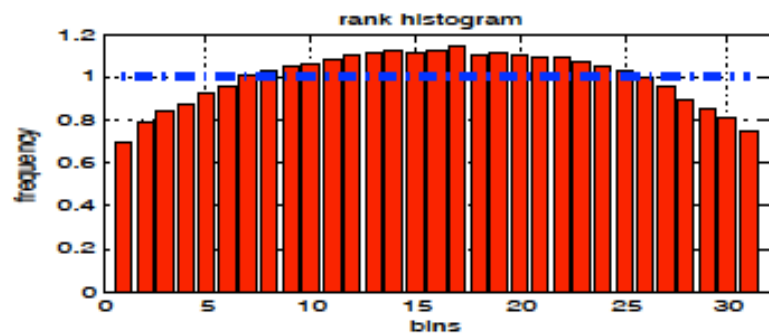
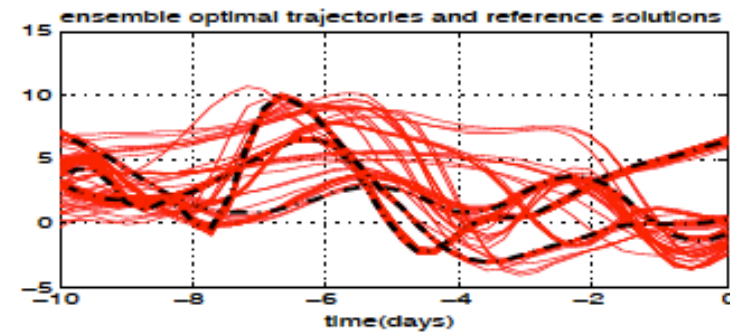
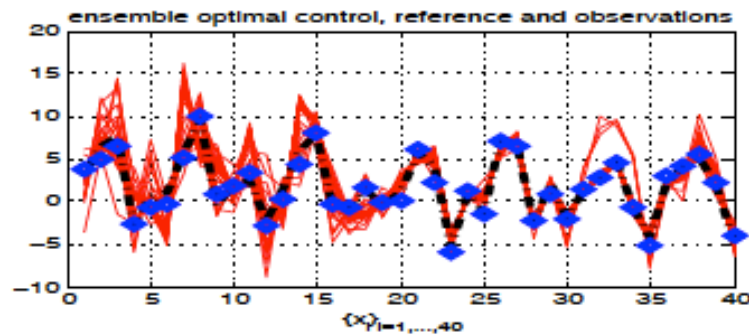


Nonlinear Lorenz'96. 5 days

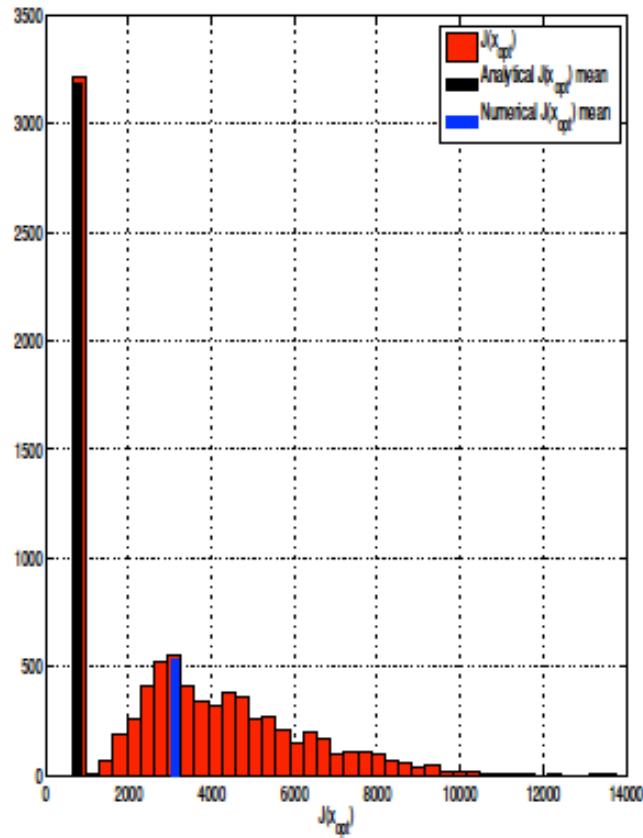


Nonlinear Lorenz'96. 5 days. Histogram of J_{min}

EnsVar : the non-linear Lorenz96 model (10 days \simeq 2 TU)

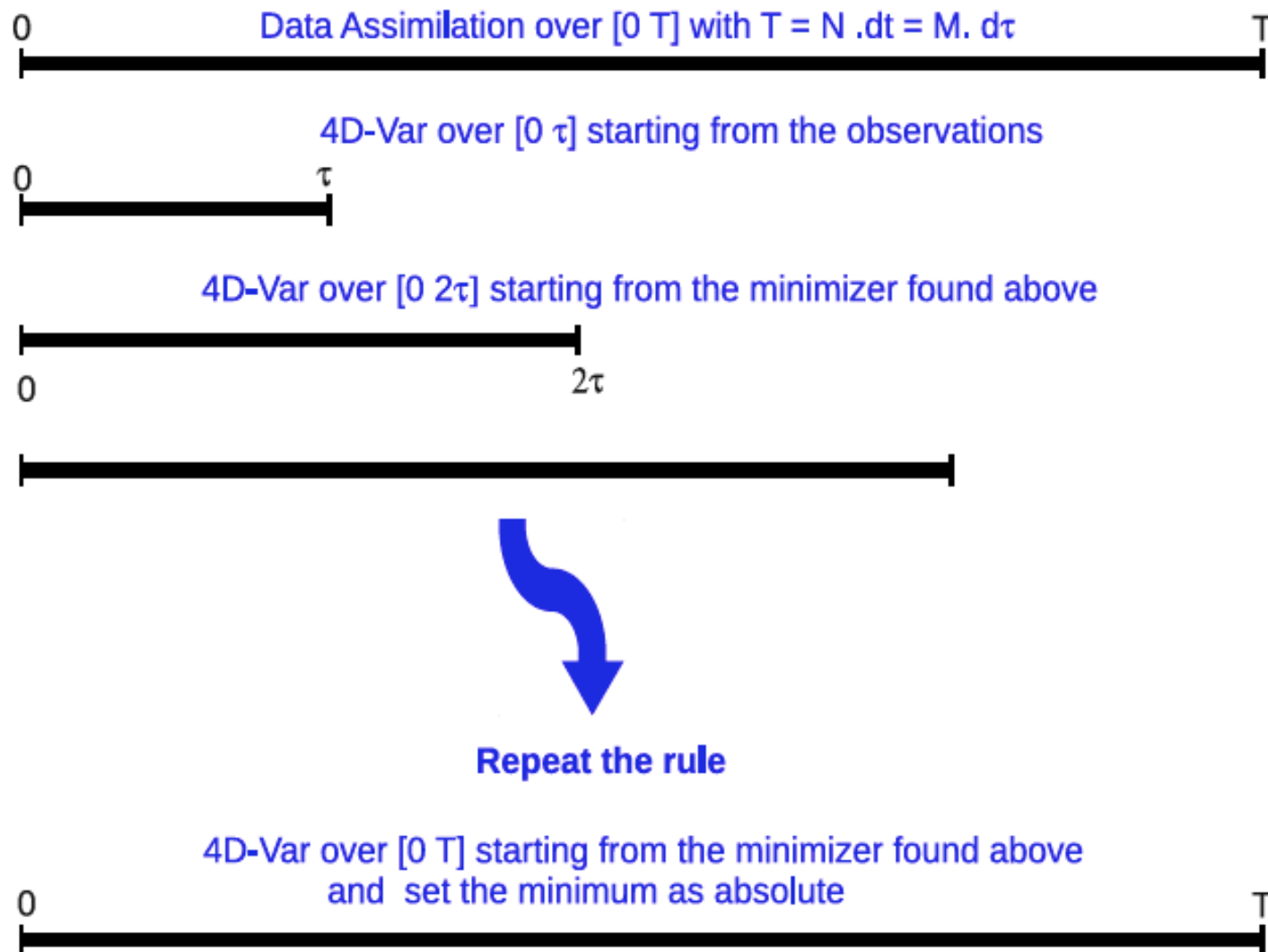


EnsVar : consistency

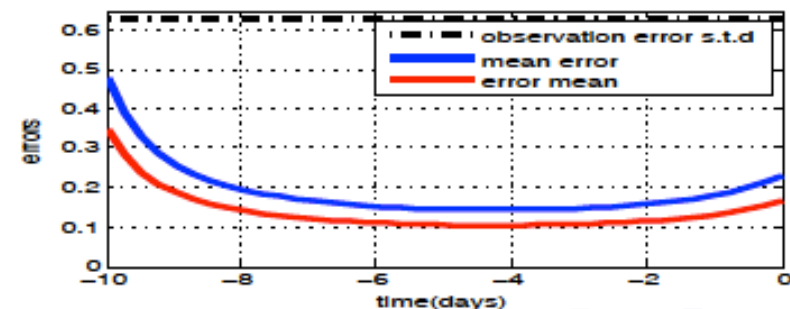
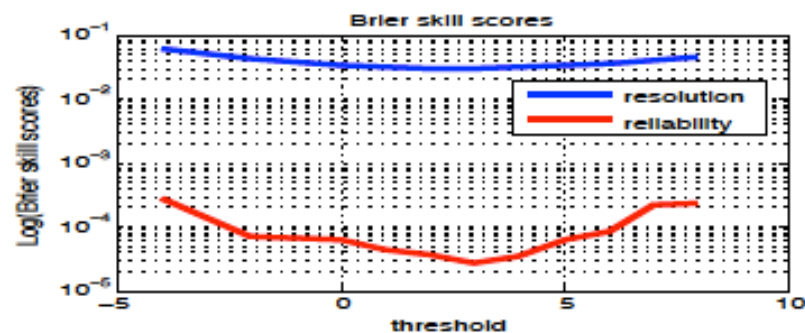
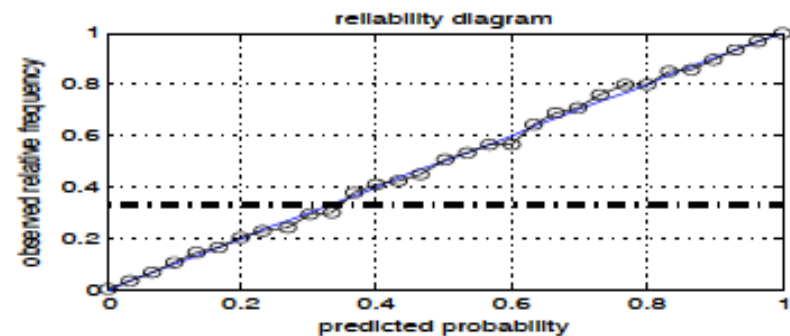
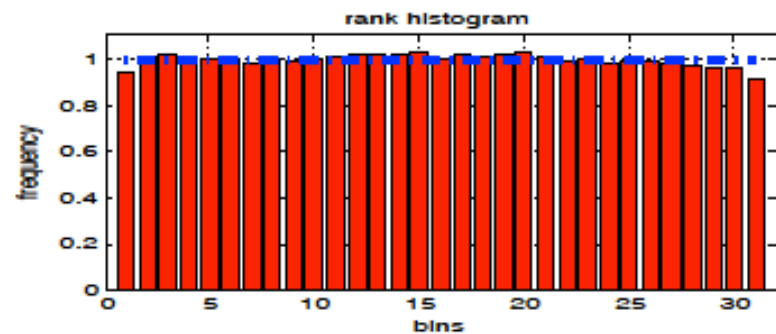
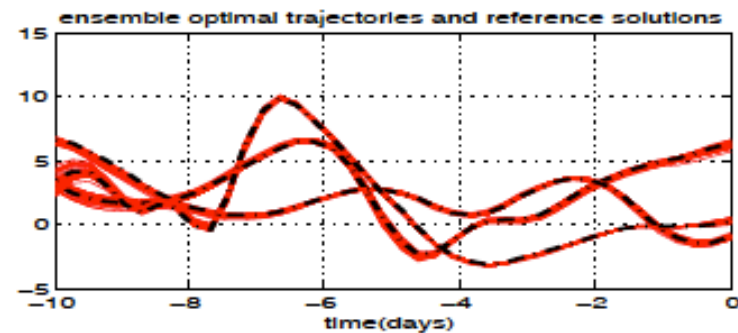
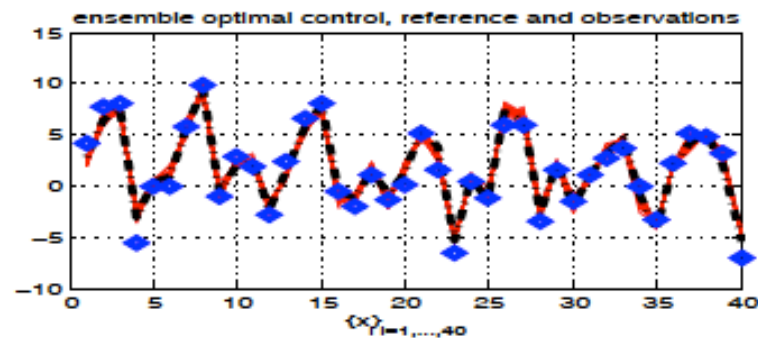


Nonlinear Lorenz'96. 10 days. Histogram of J_{min}

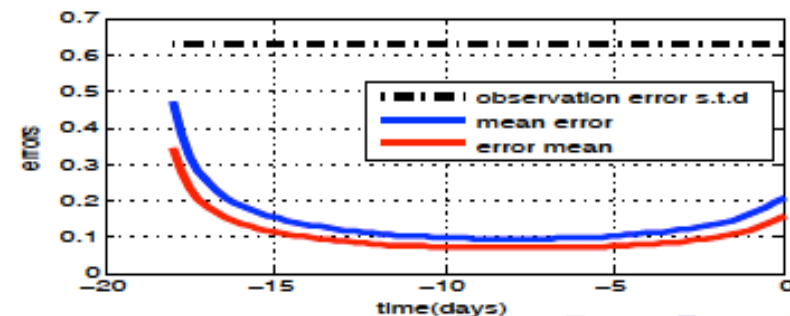
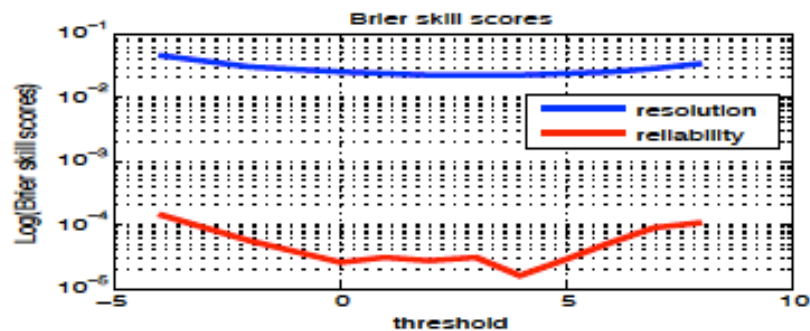
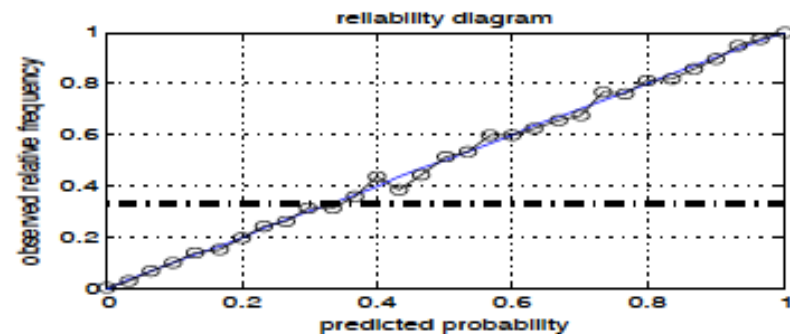
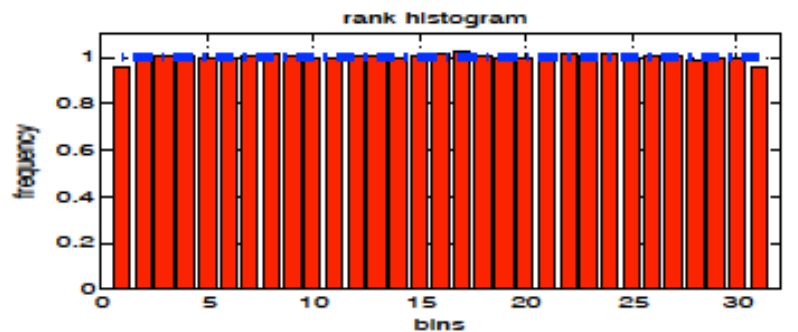
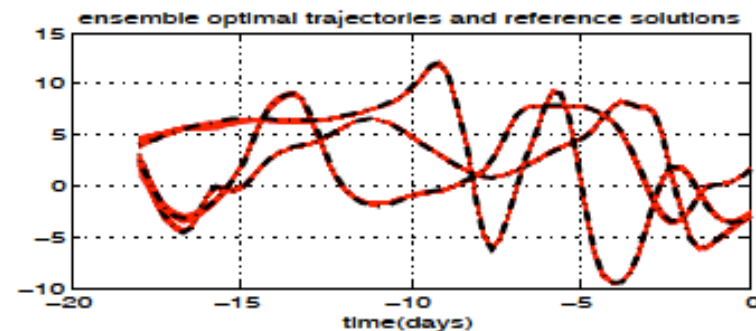
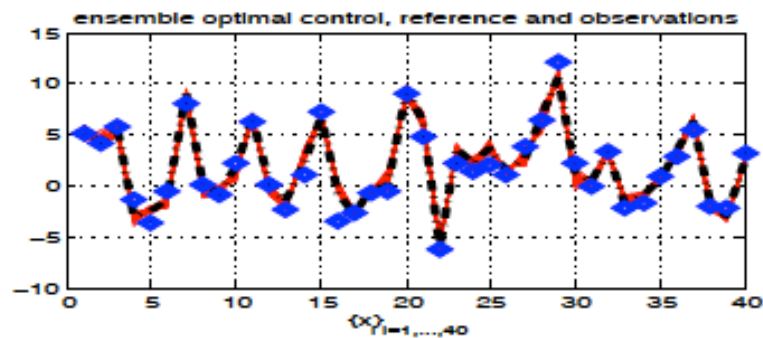
Quasi-Static Variational Assimilation (QSVA)



EnsVar : the non-linear Lorenz96 model 10 days with QSVA

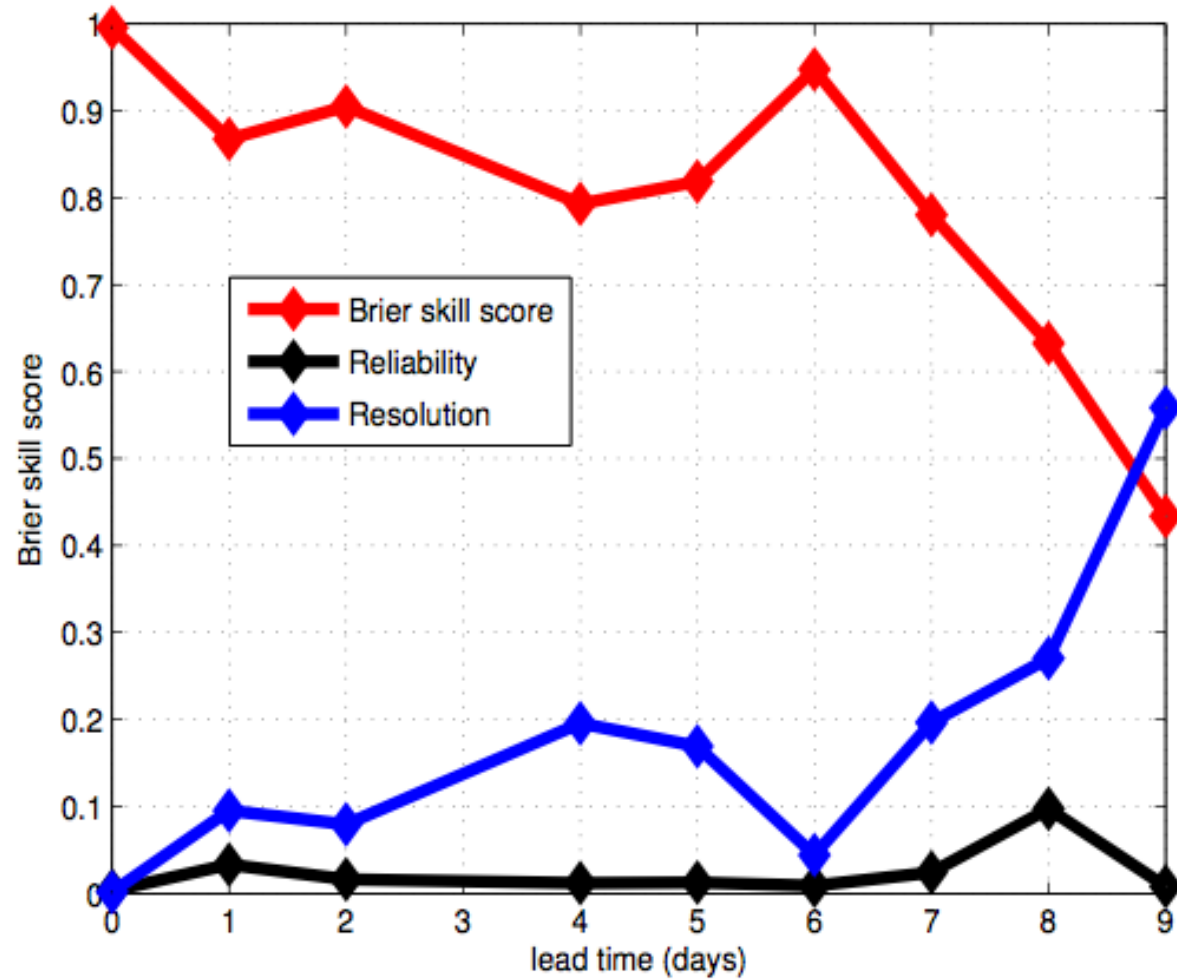


EnsVar : the non-linear Lorenz96 model 18 days with QSVA



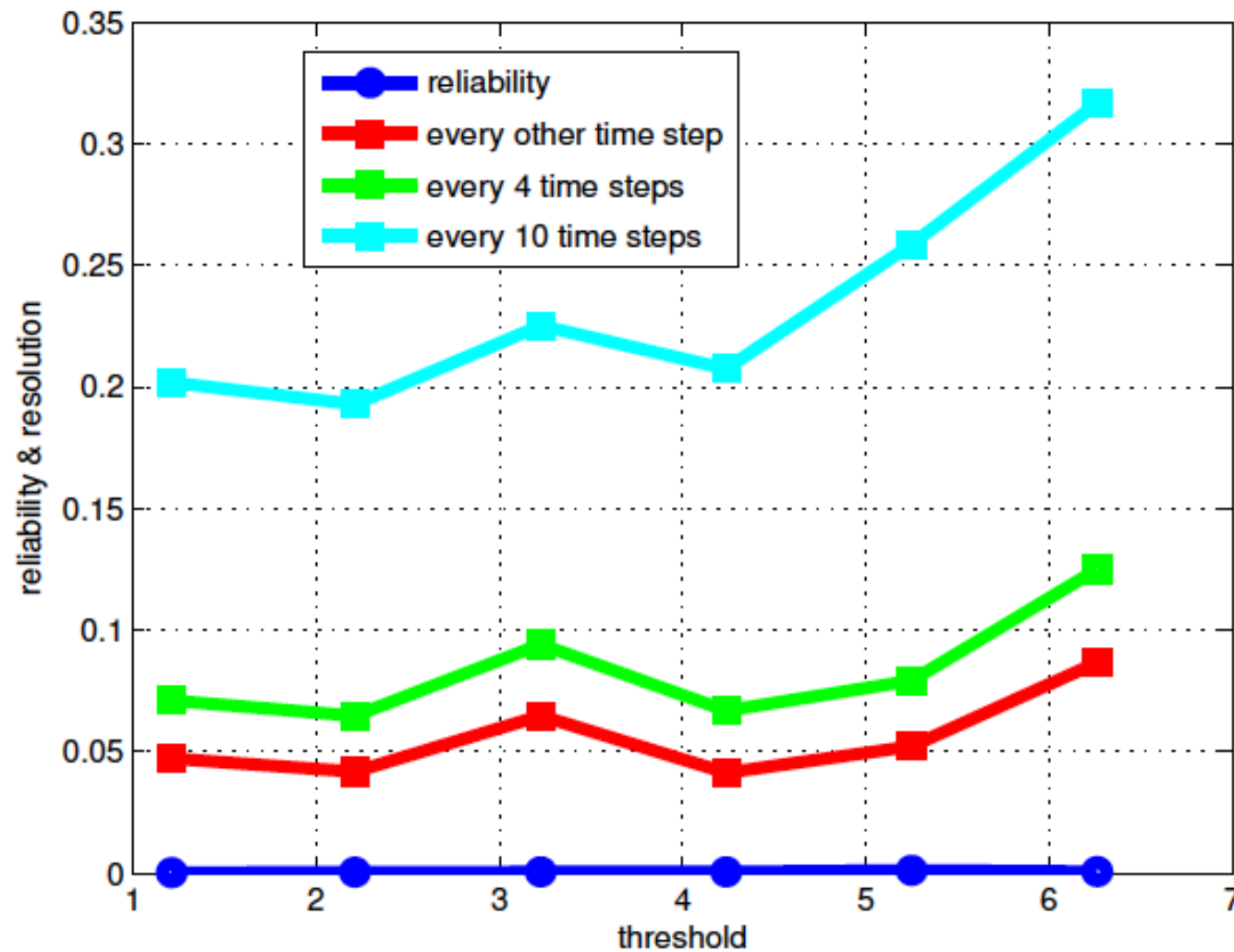
EnsVar : forecasting

Brier Skill Scores as a function of the lead time



EnsVar : observation frequency impact

Impact on the reliability and resolution

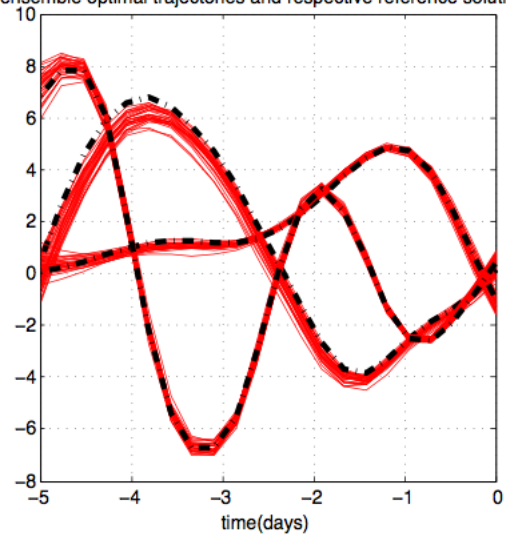


- Results are independent of the Gaussian character of the observation errors (trials have been made with various probability distributions)
- Ensembles produced by EnsVar are very close to Gaussian, even in strongly nonlinear cases.

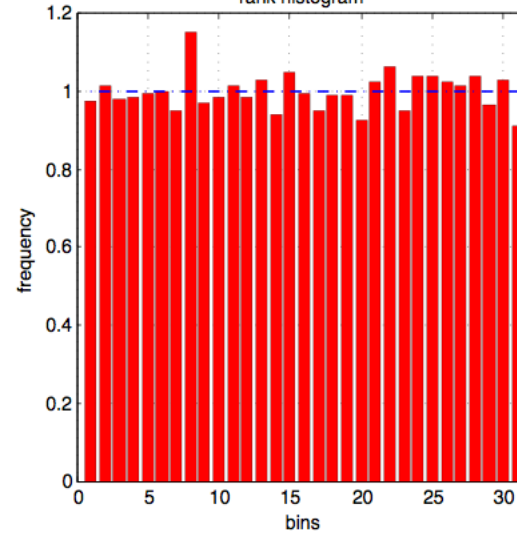
- Comparison *Ensemble Kalman Filter (EnKF)* and *Particle Filters (PF)*

Both of these algorithms being sequential, comparison is fair only at end of assimilation window

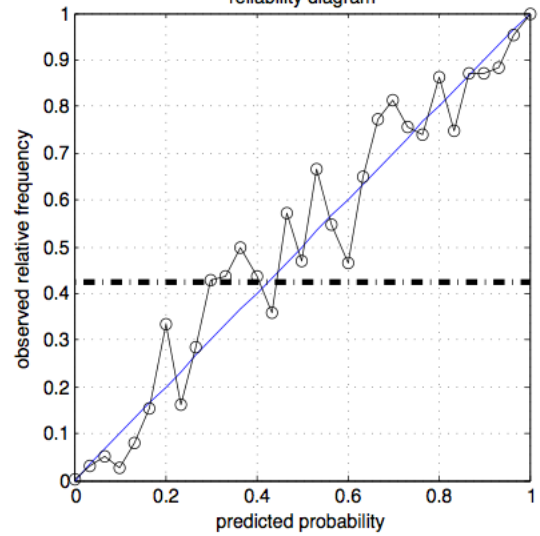
ensemble optimal trajectories and respective reference solutions



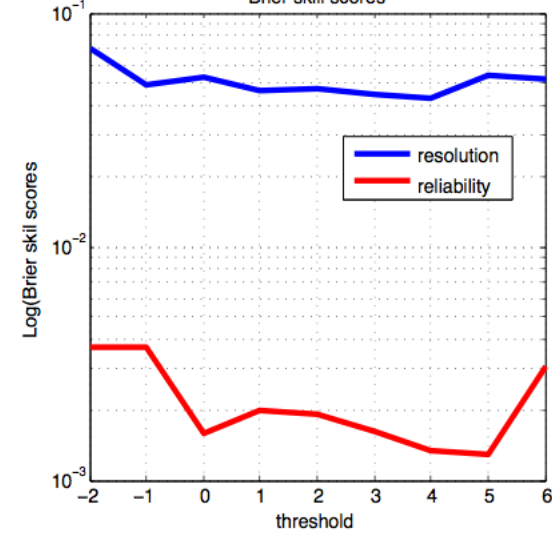
rank histogram

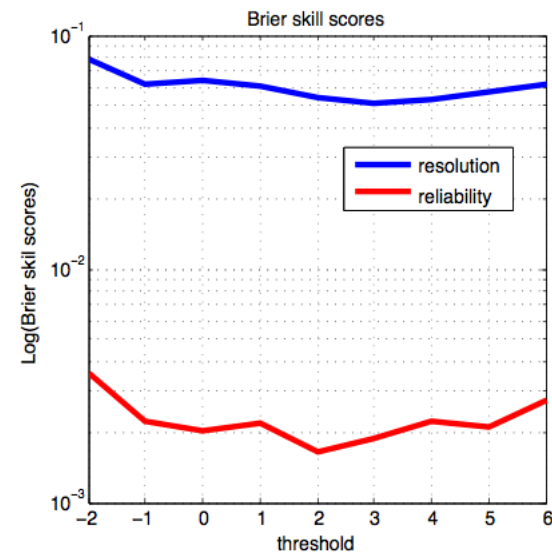
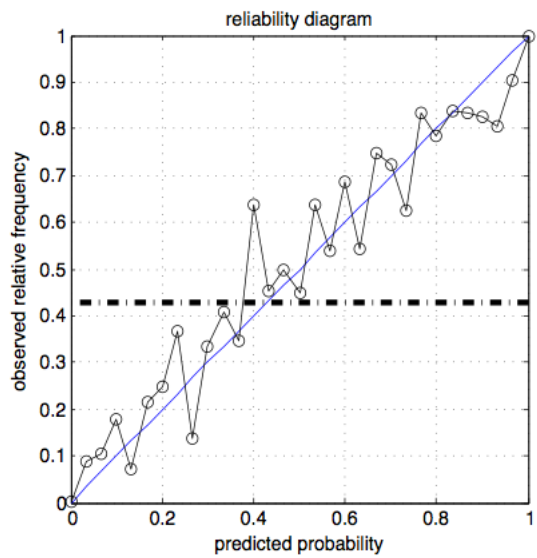
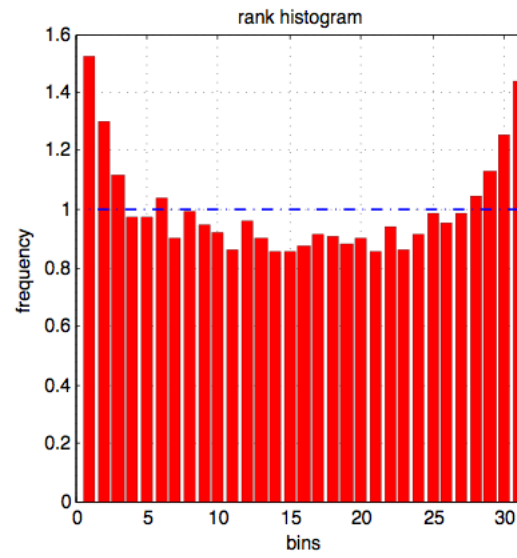
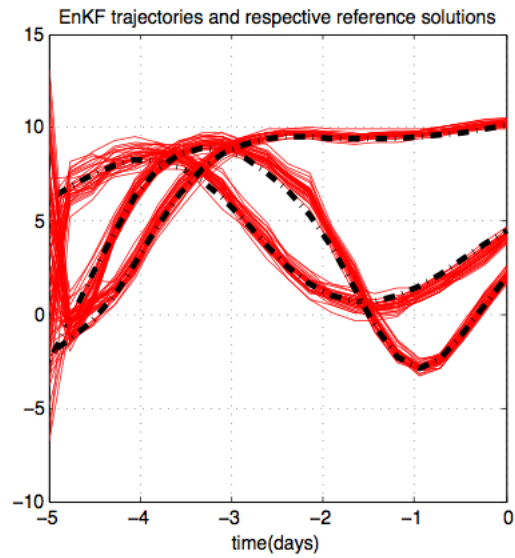


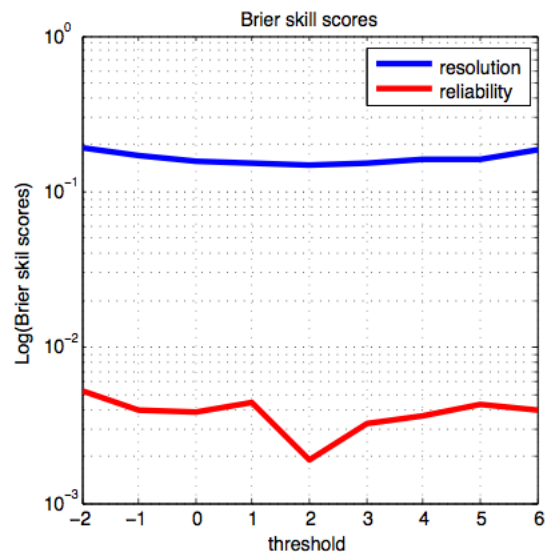
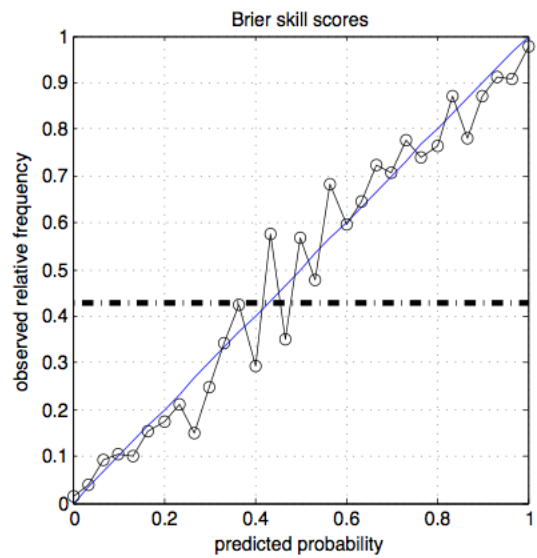
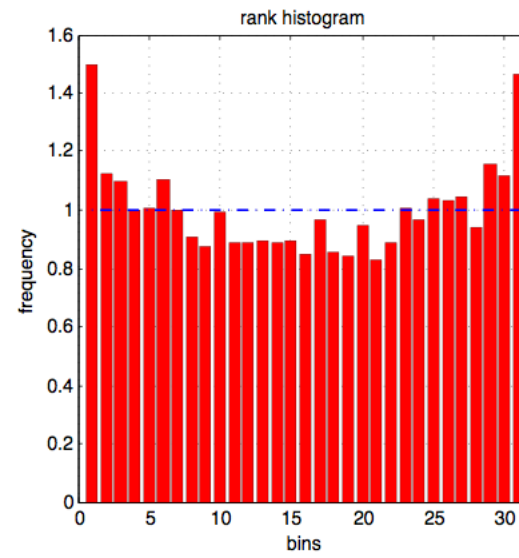
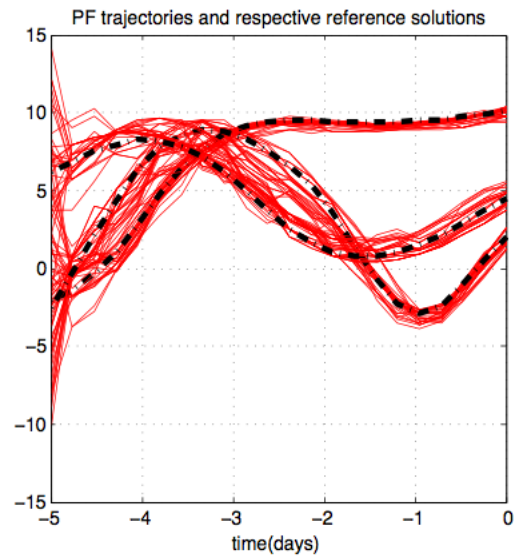
reliability diagram



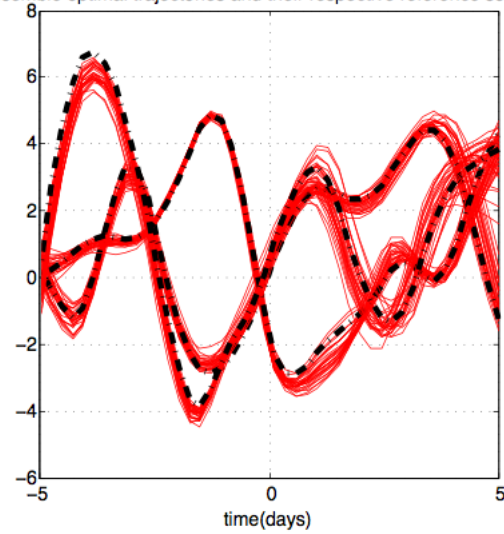
Brier skill scores



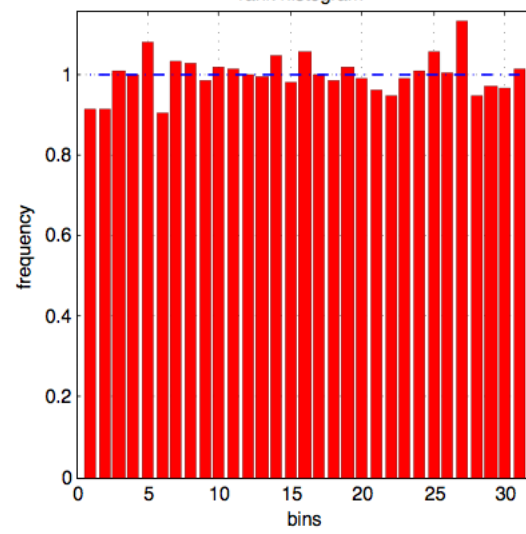




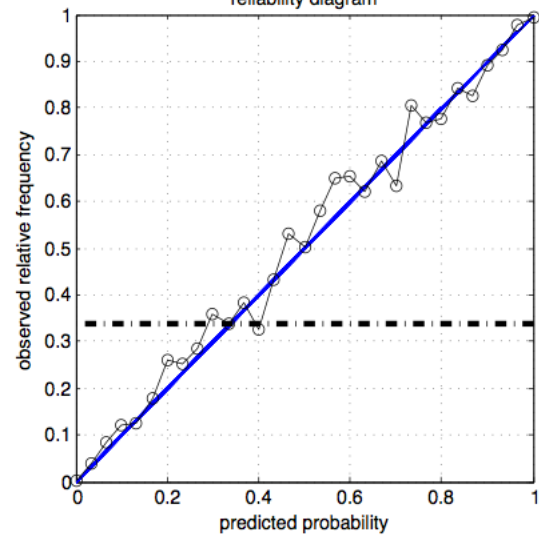
ensemble optimal trajectories and their respective reference solutions



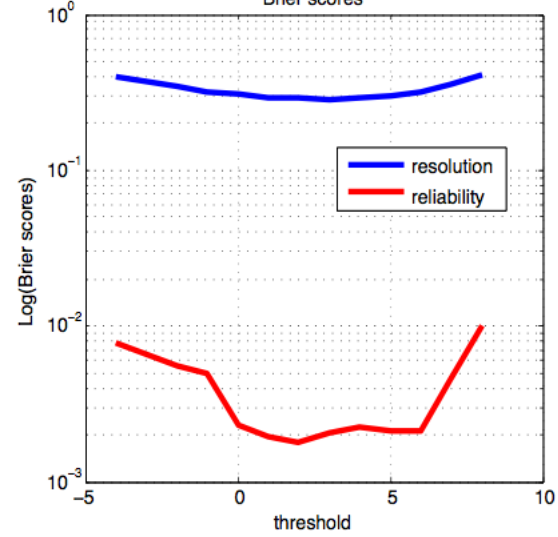
rank histogram



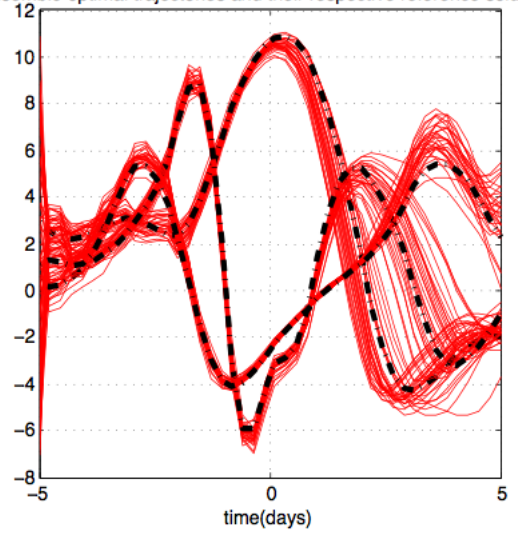
reliability diagram



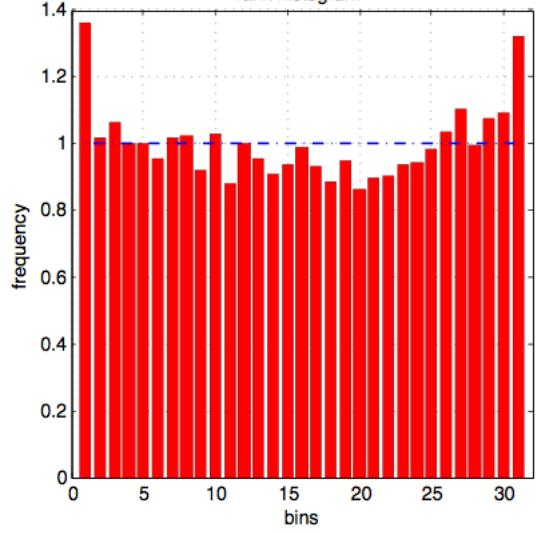
Brier scores



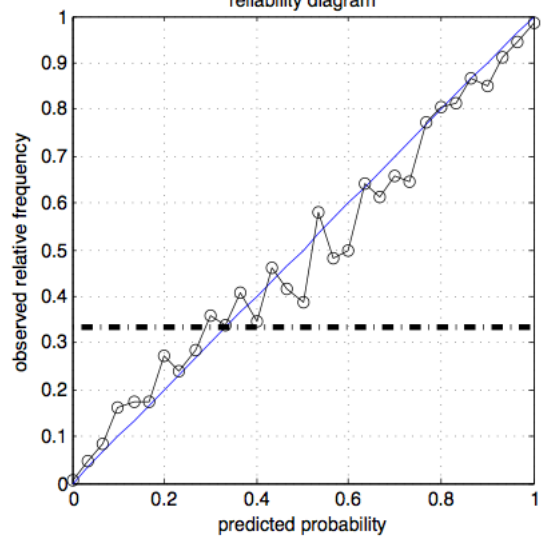
ensemble optimal trajectories and their respective reference solutions



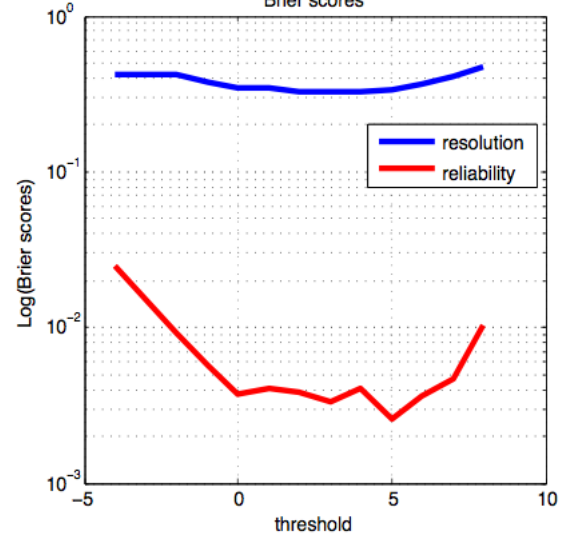
rank histogram



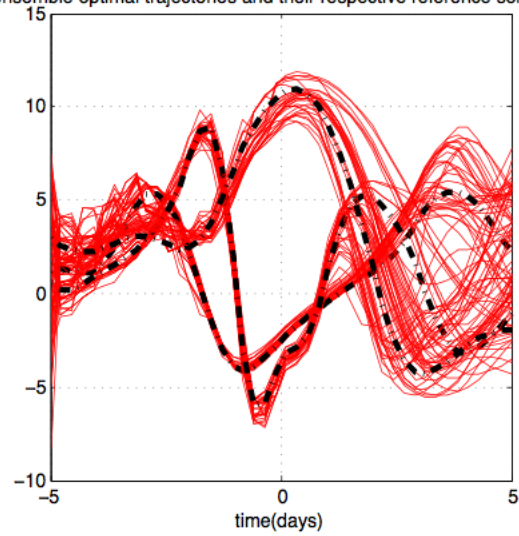
reliability diagram



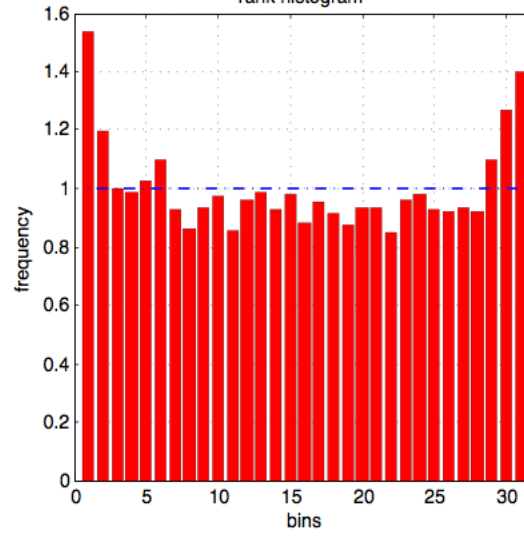
Brier scores



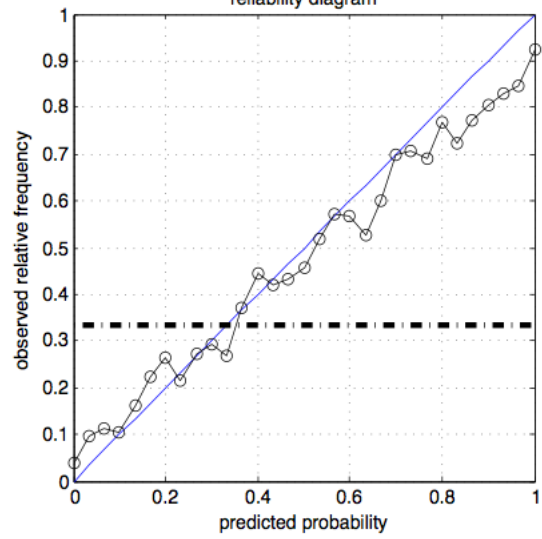
ensemble optimal trajectories and their respective reference solutions



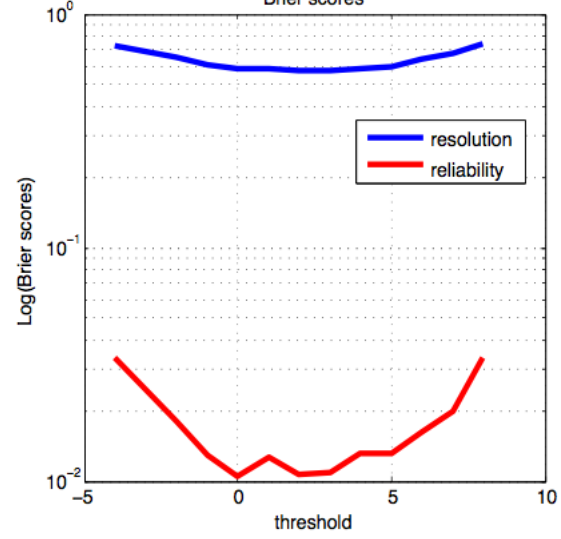
rank histogram



reliability diagram



Brier scores



<i>method</i>	<i>DA procedure</i>	<i>Assimilation</i>	<i>Forecasting</i>
EnsVAR		0.2193510	1.49403506
EnKF		0.2449690	1.67176110
PF		0.7579790	2.62461295

RMS errors at the end of 5-day assimilations and 5-day forecasts

Weak constraint EnsVar

- define the objective function.

$$\mathfrak{J}(x, \eta_1, \eta_2, \dots, \eta_{N-1}, \eta_N) = \frac{1}{2} \left\{ (x - x_b)^T \mathbf{B}^{-1} (x - x_b) \right\} +$$

$$\frac{1}{2} \sum_{i=0}^N \left\{ (y_i - H_i(x_i))^T \mathbf{R}_i^{-1} (y_i - H_i(x_i)) \right\} + \frac{1}{2} \sum_{i=1}^N \eta_i^T \mathbf{Q}_i^{-1} \eta_i$$

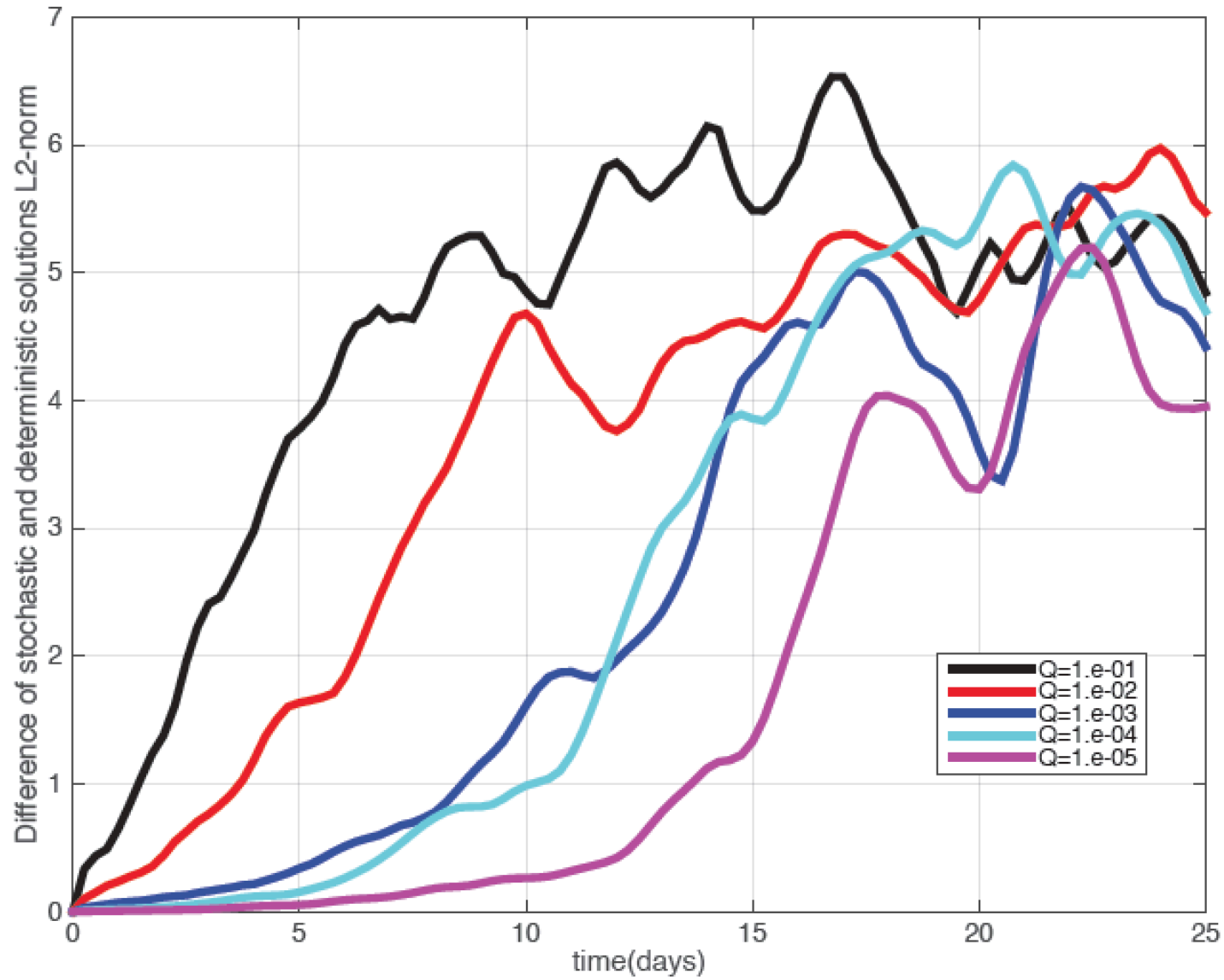
- 1 \mathbf{B} background error covariance matrix and \mathbf{R} observation error covariance matrix.
 - 2 \mathbf{Q} model error covariance matrix.
 - 3 $H : \mathbb{R}^{state} \rightarrow \mathbb{R}^{obs}$ observation operator.
 - 4 x_b background state vector and y_i observation vector at time $t = t_i$.
 - 5 η_i model error vector at $t = t_i$ with $x(t_i) = \mathfrak{M}_{t_i \leftarrow t_{i-1}}(x(t_{i-1})) + \eta_i$
- find the optimal control variable $(x_0^{opt}, \eta_1^{opt}, \eta_2^{opt}, \dots, \eta_N^{opt})$ and the optimal trajectory x^{opt} .

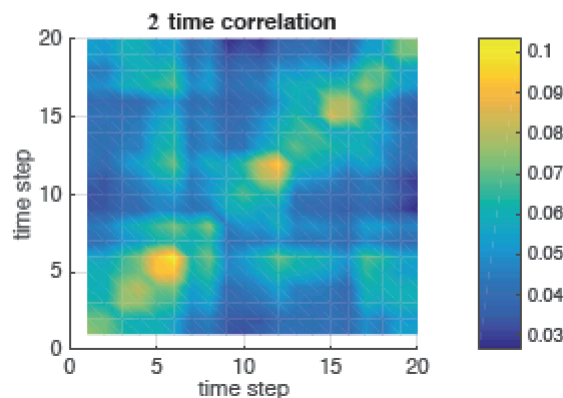
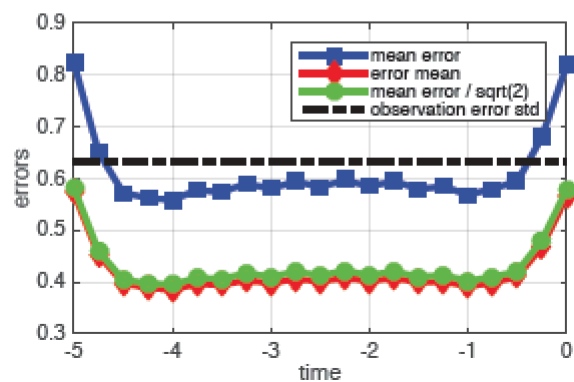
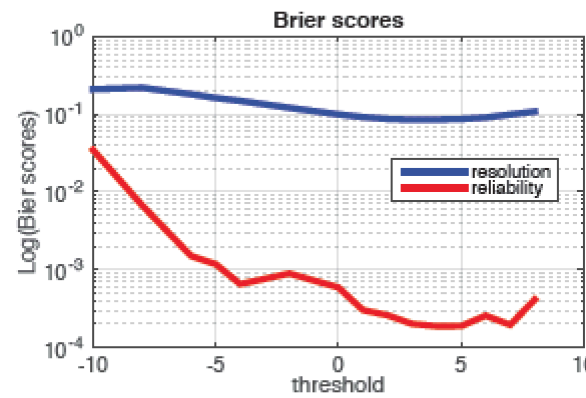
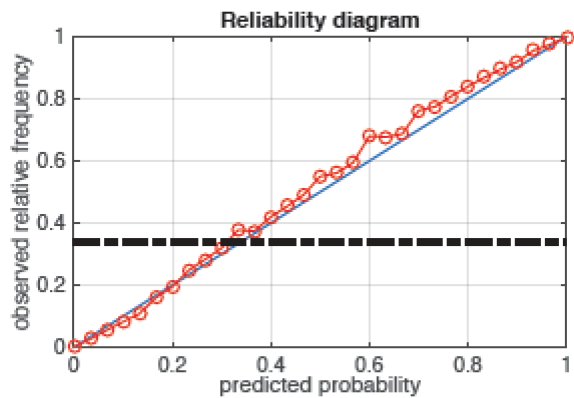
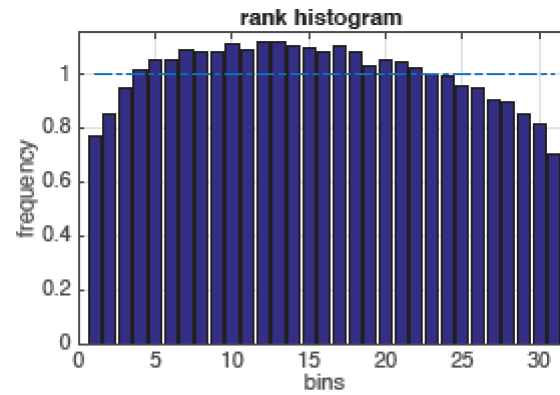
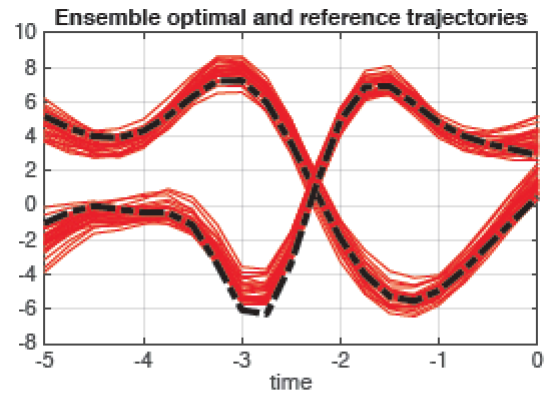
$$(x_0^{opt}, \eta_1^{opt}, \eta_2^{opt}, \dots, \eta_N^{opt}) = \min_{x, \eta_1, \eta_2, \dots, \eta_N \in \mathfrak{A}} \mathfrak{J}(x, \eta_1, \eta_2, \dots, \eta_N)$$

$$x_i^{opt} = \mathfrak{M}_{t_i \leftarrow t_{i-1}} \left(\mathfrak{M}_{t_{i-1} \leftarrow t_{i-2}} \left(\dots \left(\mathfrak{M}_{t_2 \leftarrow t_1} \left(\mathfrak{M}_{t_1 \leftarrow t_0} (x_0^{opt}) + \eta_1^{opt} \right) + \eta_2^{opt} \right) \dots + \eta_{i-1}^{opt} \right) + \eta_i^{opt} \right.$$



Divergence between stochastic and deterministic solutions



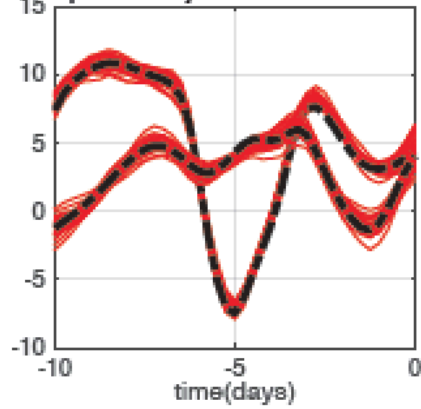


Weak EnsVar

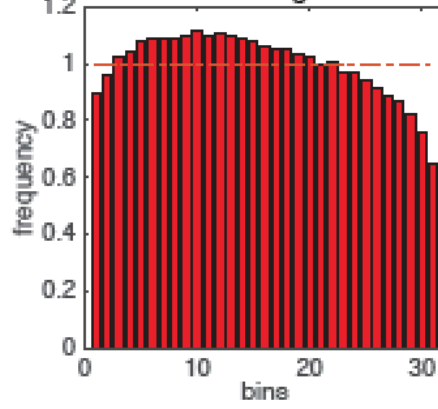
$Q = 0.1$

5-day assimilation

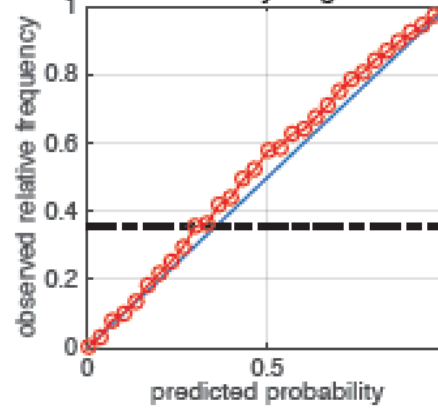
optimal trajectories and reference solution



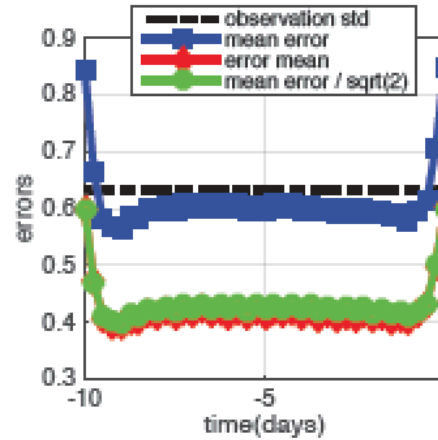
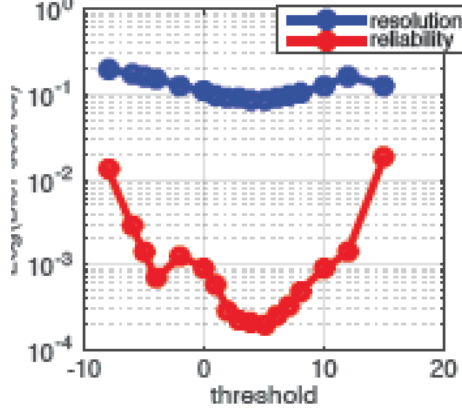
rank histogram



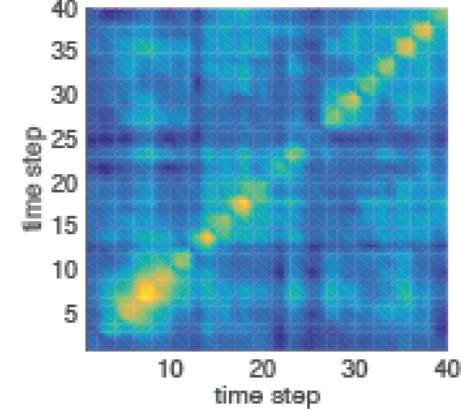
Reliability diagram



Brier scores



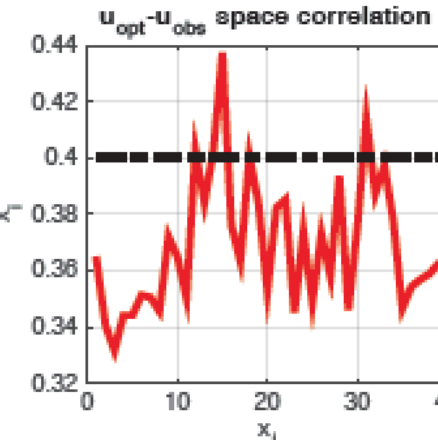
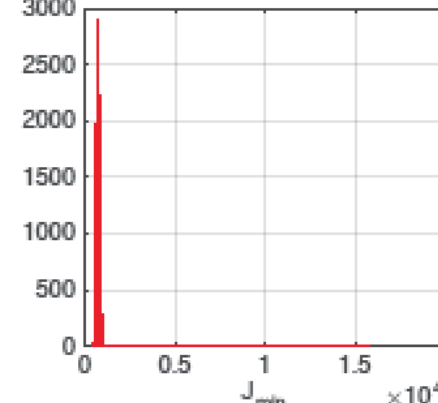
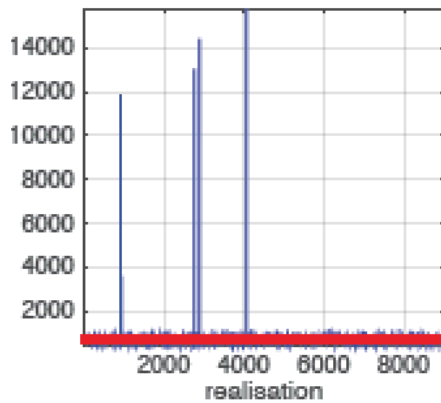
eta time correlation



Weak EnsVar

$Q = 0.1$

10-day
assimilation



Summary

- Under non-linearity and non-Gaussianity the EnsVar is a reliable and consistent ensemble estimator (provided the QSVA is used for long DA windows) .
- EnsVar is at least as good an estimator as EnKF and PF.
- Similar results have been obtained for the Kuramoto-Sivashinsky model.

Ensembles obtained are Gaussian, even if errors in data are not

Produces Monte-Carlo sample of (probably not) bayesian pdf

EnsVar : Pros and cons

Pros

- Easy to implement when having a 4D-Var code
- Highly parallelizable
- No problems with algorithm stability (i.e. no ensemble collapse, no need for localization and inflation, no need for weight resampling)
- Propagates information in both ways and takes into account temporally correlated errors

Cons

- Costly (Nens 4D-Var assimilations).
- Empirical.
- Cycling of the process (**work in progress**).

And now ?

- Implementation on physically more realistic models (QG, Shallow water, ...)
- Comparison with other ensemble algorithms (IEnKS)
- Cycling and/or overlap
- Minimisation in unstable space (AUS, Trevisan *et al.*)
- ...

The End